procesy technologiczne, obróbka powierzchniowa, warstwa wierzchnia, kontakt nieliniowy, modelowanie, metoda elementu skończonego, równania dyskretne, metoda explicit, analiza numeryczna
technological processes, metal forming, surface layer, nonlinear contact, modelling, Finite Element Method, discretized model, dynamic explicit method, numerical analysis

Leon KUKIEŁKA[1]
Krzysztof KUKIEŁKA[2]

MODELLING AND ANALYSIS OF THE TECHNOLOGICAL PROCESSES USING FINITE ELEMENT METHOD

Paper presents the problem of modelling and analysis of metalworking processes. Technological processes were considered as a geometrical, physical and thermal boundary and initial value problem, with unknown boundary conditions in the contact zone. An incremental model of the contact problem between movable rigid or thermo-elastic body (tool) and thermo-elastic/thermo-visco-plastic-phases body (object) in updated Lagrange formulation, for spatial states (3D) was considered. The incremental functional of the total energy and variational, non-linear equation of motion of object and heat transfer on the typical step time were derived. This equation has been discretized by finite element method, and the system of discrete equations of motion and heat transfer of objects were received. For solution of these equations the explicit or implicit methods was used. The applications were developed in the ANSYS/LS-Dyna system, which makes possible a complex time analysis of the states of displacements, strains and stresses, in the workpieces in fabrication processes. Application of this method was showed for examples the modelling and the analysis of burnishing rolling, thread rolling and turning processes. The numerical result were verified experimentally.

MODELOWANIE I ANALIZA PROCESÓW TECHNOLOGICZNYCH METODĄ ELEMENTU SKOŃCZONEGO

W artykule przedstawiono problematykę modelowania i analizy numerycznej procesów technologicznych obróbki metali. Proces te rozpatrzono jako geometrycznie, fizycznie i cieplnie nieliniowe zagadnienie brzegowo-początkowe, z nieznanymi warunkami brzegowymi w obszarze kontaktu. Do opisu zjawisk nieliniowych, na typowym kroku przyrostowym, wykorzystano uaktualniony opis Lagrange'a, traktując narzędzie jako ciało sztywne lub termo-sprężyste natomiast przedmiot jako ciało termo-sprężyste/termo-lepko-plastyczne-fazowe. Równania ruchu obiektu i ciepła wyprowadzono wykorzystując rachunek wariacyjny. Otrzymane równania wariacyjne dyskretyzowano stosując aproksymację właściwą metodzie elementu skończonego. Dyskretne równania rozwiązano stosując jawne metody całkowania. Opracowano aplikacje w systemie ANSYS/LS-Dyna, które pozwalają na kompleksową analizę stanów przemieszczeń, odkształceń, naprężeń w dowolnym miejscu ciała i w dowolnej chwili realizacji procesu obróbki. Przedstawiono przykładowe wyniki obliczeń numerycznych stanów naprężeń i odkształceń wybranych procesów technologicznych: nagniatania, walcowania gwintów i toczenia. Wyniki obliczeń numerycznych weryfikowano eksperymentalnie.

1. INTRODUCTION

The dynamic development of technology means that the greater are the requirements that are put before modern machines and equipment; even greater are the requirements in respect of durability and reliability of associated units which, in certain operational conditions, constitute tribological systems.

Improper physical and stereometrical properties of the surface layer cause the failure damage in approximately 85% of modern machine units; they also influence the decrease in life and the increase of energy consumption to overcome frictional resistance. Nowadays, about 50% of the energy supplied is lost in the friction of elements in relative motion [1, 2]

Thus, one of the most important technological problems in the manufacturing and in the recovery of elements is the formation of the surface layer, characterized by assigned physical and stereometrical properties and precision in dimension and form, that affects the target life and the reliability of the machined elements. Special

[1] Politechnika Koszalińska, Wydział Mechaniczny, 75-620 Koszalin, ul. Racławicka 15-17, tel: + 48 881-583-045, e-mail: leon.kukielka@tu.koszalin.pl
[2] Politechnika Koszalińska, Wydział Mechaniczny, 75-620 Koszalin, ul. Racławicka 15-17, tel: + 48 791-585-363, e-mail: krzysztof.kukielka@tu.koszalin.pl

attention should be paid to those machine elements which are costly to manufacture, or which have a bearing on machine reliability and environmental pollution, etc.

Knowledge of the guillotining process is based mainly on experimental methods, which are often expensive and unable to be extrapolated to other cutting configurations. Therefore, computational models, such as the finite element method (FEM), are valuable in reducing the number of trial-and-error experiments required to predict the state of material displacement, residual stresses, strains, material fracture, sheet deformations and quality of the sheared edge.

Numerical analysis is a valuable tool to extend the period of time and knowledge of phenomena whose experimental researches is difficult or impossible. These are mainly phenomena occurring in extremely small areas, running at high speeds, existing in a very short time, and determining the results of the treatment process. For such problems, in particular:

– friction, adhesion and slip,
– displacement, strain, stress and temperature in the surface layer of the workpiece,
– variability tool contact areas with the object and boundary conditions,
– variability of the workpiece during machining.

Understanding the effect of the treatment on the state of strain, stress and temperature in the surface layer of the workpiece is important for the correct design of the process.

One major steps to achieve effective solutions to the Finite Element Method is to develop a universal model of the investigated process. At Department of Technical Mechanics at the Faculty of Mechanical Engineering of the Koszalin University of Technology were developed applications on the system ANSYS (APDL language), which allow a comprehensive time analysis for deformation (displacement, velocity, strain, strain rate), stresses and boundary condition in contact zone tool-object occurring in the object, both the spatial conditions as well as plane, in the processes technological precision machining parts (Fig. 1): cutting processes [8, 36, 37, 38, 45, 47, 55, 56, 62, 63, 66, 74], turning processes [20, 34, 57, 75], burnishing rolling processes [1, 2, 3, 6, 7, 11, 17, 22, 28, 29 ,31-33, 36, 46, 49, 51, 60, 61, 65, 71, 73, 76-78], sliding burnishing [43, 53, 57, 58, 68], cutting by an abrasive single grain [12, 14, 19, 21, 24, 25, 33, 39, 40, 72], embossing [12, 23, 30, 50, 70], thread rolling [1, 2, 4, 5, 9, 10, 13, 15, 16, 18, 26, 35, 41, 44, 48, 54, 67], duplex burnishing [13, 14, 36], drawing [27, 52, 69] and shot penning [42, 59, 64]. In applications were used a theoretical bases processes precision machining of modern parts, developed in [3, 6, 7, 15, 26, 27, 28, 31, 39, 40-42, 46].

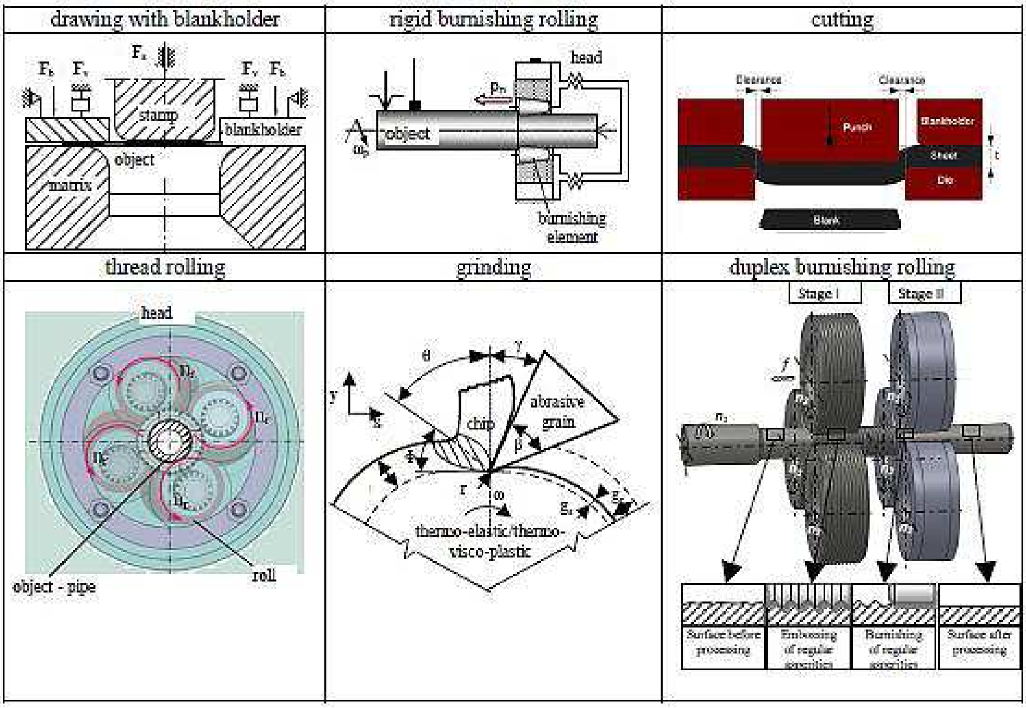

Fig. 1. Schema of precision machining of modern parts

The latest trend in the modelling and analysis processes is the numerical modelling using Finite Element Method (FEM). It involves replacing the continuous object (the real) discrete object with separate sub-volumes and/or sub-areas – finite elements containing a finite number of nodes. The development of the computational capabilities of computers and software allows analysis of modern technological processes precision machining of parts using computer programs using FEM [79-81] and iterative calculation using the updated Lagrangian description [79].

Numerical analysis is a valuable tool for understanding phenomena that experimental study is difficult or impossible. These are mainly phenomena occurring in extremely small areas, running at high speeds, lasting a very short time and determining the results of the sliding cutting or burnishing. Until such problems are, in particular friction, adhesion and slip, movements, strain, stress and temperature of the workpiece, the workpiece variability of cracking material. Numerical analysis also allows to determine the impact of technology on the quality of the product: the type of material and its state, geometry tools, the effect of processing conditions on the state of strain, stress and temperatures in the subject, shapes burrs, chips, quality surface finish.

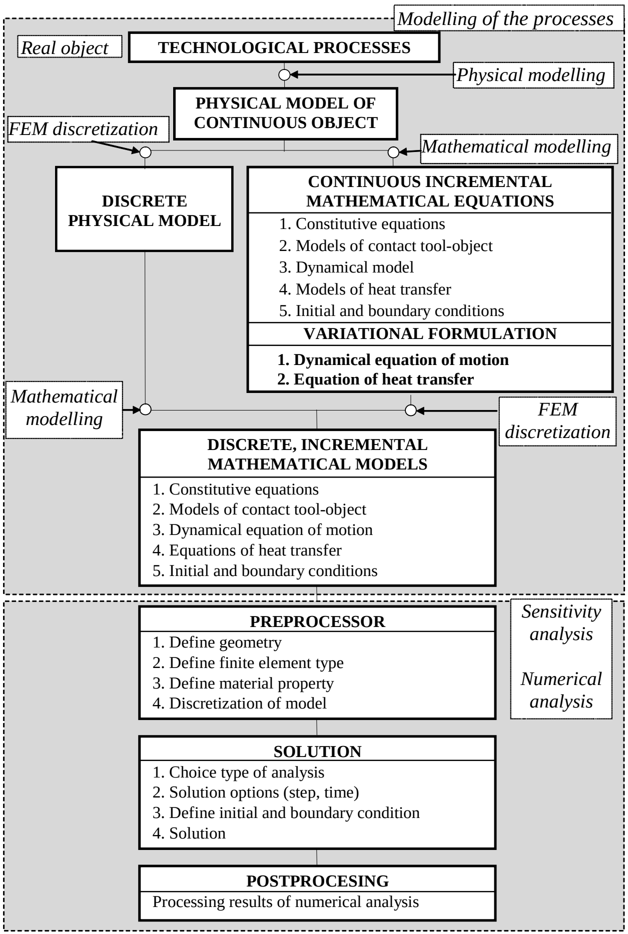

Fig. 2. *Schema of modern modelling and numerical analysis of technological processes and its implementation for the treatment of machine parts*

Knowledge of the physical phenomena occurring in the material, in areas where the tool is in contact with the object while the technological processes are carried out, is a basic necessity. It also enables the control of the properties of the surface layer of the product and the achieving of the greatest shape-dimensional accuracy. Thus, one of the most important technological problems in the metal forming processes is the calculation of displacement, strain and stress in the surface layer. The objective in this paper is to present the modern method to modelling, analysis and testing of a solution procedure for the geometrical, physical and thermal non-linear analysis of thermo-elastic/thermo-visco-plastic-phases behaviour with/without temperature-dependent material properties (Fig. 2).

The incremental mathematical model of technological processes, in the updated Lagrange formulation, contain the constitutive equations (model of dynamical yield stress, thermo-elastic/thermo-visco-plastic-phases strains model, thermo-elastic/thermo-visco-plastic-phases stress model), the model of contact between tool-workpiece, dynamic equation of motion and deformation, equations of heat transfer, initial and boundary conditions. First, variational method developed equation of motion and deformation for a typical step time. Then, equation with Finite Element Method (FEM) was discretized, given the equations of motion and deformation and head transfer of a discrete object. Then, the explicit (DEM) or implicit (DIM) schemes to step by step numerical solution are adopted. The algorithms of numerical analysis in ANSYS program for different technological processes were elaborated [8, 12, 14-24, 29-34, 36-43, 46-59, 62-78], where discrete equation was applied together with initial and boundary conditions.

2. CONTINUOUS INCREMENTAL MATHEMATICAL EQUATIONS

The incremental mathematical model of technological processes, in the updated Lagrange formulation, for typical step time $t \to \tau = t + \Delta t$, contain the constitutive equations (model of thermo-dynamical yield stress, thermo-elastic/thermo-visco-plastic-phases stains model, thermo-elastic/thermo-visco-plastic-phases stress model), the model of contact between tool-workpiece, dynamic equation of motion and deformation, model of heat transfer and initial and boundary conditions.

2.1. Incremental model of thermo-dynamic yield stress

Yield stress σ_Y is the most important parameter characterizing the resistance of a thermo-visco-plastic deformation. The incremental model of yield stress for typical step time $t \to \tau = t + \Delta t$, is defined as [6, 7, 39, 40]:

$$\begin{aligned}\Delta\sigma_Y = {} & F_1(y)\cdot\Delta y + \frac{\partial F_2(\cdot)}{\partial \sigma_{st}}\cdot F_3(\varepsilon_{eq}^{(VP)})\cdot\Delta\varepsilon_{eq}^{(VP)} + \frac{\partial F_2(\cdot)}{\partial \dot{\varepsilon}_{eq}^{(VP)}}\cdot \Delta\dot{\varepsilon}_{eq}^{(VP)} + \\ & + \frac{\partial F_2(\cdot)}{\partial T}\cdot \Delta T + \frac{\partial F_2(\cdot)}{\partial \sigma_{st}}\cdot F_4(t)\cdot\Delta t,\end{aligned} \tag{1}$$

where $\Delta\varepsilon_{eq}^{(VP)}$ and $\Delta\dot{\varepsilon}_{eq}^{(VP)}$ are the increment of effective visco-plastic strain and strain rate, respectively, σ_{st} is state stress depending of the accumulated effective visco-plastic strain and time t, $F_1(y)\cdot\Delta y$ is the component of change in the initial yield stress σ_0 with a change of chemical composition; $[\partial F_2(\cdot)/\partial\sigma_{st}]\cdot F_3(\varepsilon_{eq}^{(VP)})\cdot\Delta\varepsilon_{eq}^{(VP)}$ is the component of change in the temporary yield stress σ_Y with change of the visco-plastic strain, $[\partial F_2(\cdot)/\partial\dot{\varepsilon}_{eq}^{(VP)}]\cdot\Delta\dot{\varepsilon}_{eq}^{(VP)}$ is the component of change in the temporary yield stress with change of the visco-plastic strain rate, $[\partial F_2(\cdot)/\partial T]\cdot\Delta T$ is the component of change in the temporary yield stress with change of the temperature, $[\partial F_2(\cdot)/\partial\sigma_{st}]\cdot F_4(t)\cdot\Delta t$ is the component of change of a temporary yield stress with time.

2.2. Damping model

Very essential and difficult problem during modelling of technological processes is the regard the phenomenon of dissipation energy. The dissipation of energy influences on decrease of displacement and dynamic stress in object. The difficulty depends on selection of proper physical model mainly as well as qualification of suitable values of his parameters. At present [79-81] usually the Rayleigh damping is used, which damping matrix $\mathbf{C}$ is calculated from equation: $\mathbf{C} = \alpha_1\cdot\mathbf{M} + \alpha_2\cdot\mathbf{K}$, where $\mathbf{M}$ and $\mathbf{K}$ are mass and stiffness matrices, α_1 and α_2 are constants to be determined from two given damping ratios that correspond to two unequal frequencies of vibration.

In case of modelling the dynamical processes one should apply the damping models dependent from velocity, strain and strain rate. For this reason we propose calculate the dissipation energy, for typical step time, from following Eq. [31]:

$$\begin{aligned}\Delta E_d \cong {} & \alpha_1\cdot\int_V \rho\cdot\Delta\dot{u}_i\cdot\Delta u_i\cdot dV + \alpha_1\cdot\int_V \rho\cdot\Delta\dot{u}_i\cdot u_i\cdot dV + \alpha_1\cdot\int_V \rho\cdot\dot{u}_i\cdot\Delta u_i\cdot dV + \\ & + \frac{1}{2}\cdot\alpha_2\cdot\int_V C_{ijkl}^{(E)}\cdot\Delta\dot{\varepsilon}_{ij}\cdot\Delta\varepsilon_{kl}\cdot dV + \frac{1}{2}\cdot\alpha_2\cdot\int_V C_{ijkl}^{(E)}\cdot\Delta\dot{\varepsilon}_{ij}\cdot\varepsilon_{kl}\cdot dV + \\ & + \frac{1}{2}\cdot\alpha_2\cdot\int_V C_{ijkl}^{(E)}\cdot\dot{\varepsilon}_{ij}\cdot\Delta\varepsilon_{kl}\cdot dV,\end{aligned} \tag{2}$$

where $\Delta u_i, \Delta\dot{u}_i$ are the i*th* increment components of displacement and velocity vectors at typical step time Δt, respectively, u_i is accumulated i*th* component of displacement vector at time t.

2.3. Increment components of total strain and stress tensor models

The aim of this section is to present a material model which includes the combined effects of thermo-elasticity (in reversible zone) and thermo-visco-plasticity (in non reversible zone). The model takes into account the history of the strain, strain rate and temperature of material and a possibility of phase change to occur in it.

A basic assumption in the formulation of the model is that the usual small increment components $\Delta\varepsilon_{ij}$ of strain tensor $\mathbf{T}_{\Delta\varepsilon}$ can be expressed as the sum of thermo-elastic $\Delta\varepsilon_{ij}^{(TE)}$, visco-plastic $\Delta\varepsilon_{ij}^{(VP)}$, phases $\Delta\varepsilon_{ij}^{(F)}$ and thermal $\Delta\varepsilon_{ij}^{(TH)}$ increment strains:

$$\Delta\varepsilon_{ij} = \Delta\varepsilon_{ij}^{(TE)} + \Delta\varepsilon_{ij}^{(VP)} + \Delta\varepsilon_{ij}^{(TH)} + \Delta\varepsilon_{ij}^{(F)}, \tag{3}$$

where:

$$\Delta\varepsilon_{ij}^{(VP)} = \Delta\lambda \cdot \frac{\partial F}{\partial \tilde{S}_{ij}}, \tag{4}$$

$$\Delta\varepsilon_{ij}^{(TH)} \cong \alpha_m(T) \cdot \Delta T \cdot \delta_{ij}, \tag{4b}$$

$$\Delta\varepsilon_{ij}^{(F)} = \Delta\xi \cdot \delta_{ij} = \frac{(\rho_1/\rho_2) - 1}{3} \cdot \delta_{ij} \tag{4c}$$

are visco-plastic, thermal and phases strain tensor, respectively, α_m is the mean coefficient of thermal expansion, $\Delta\xi$ is the coefficient of expansion into a phase change, ρ_1 and ρ_2 are the mass densities of old and new phase,

$$\Delta\lambda = \frac{\tilde{S}_{ij} \cdot C_{ijkl}^{(E)} \cdot \Delta\varepsilon_{kl} - \frac{2}{3} \cdot \sigma_Y(\varepsilon_{eq}^{(VP)}, \dot{\varepsilon}_{eq}^{(VP)}, T) \cdot \dot{E}_T \cdot \Delta\dot{\varepsilon}_{eq}^{(VP)}}{\tilde{S}_{ij} \cdot C_{ijkl}^{(E)} \cdot \tilde{S}_{kl} + \frac{2}{3} \cdot [\sigma_Y(\varepsilon_{eq}^{(VP)}, \dot{\varepsilon}_{eq}^{(VP)}, T)]^2 \cdot [\tilde{C}(\varepsilon_{eq}^{(VP)}, \dot{\varepsilon}_{eq}^{(VP)}, T) + \frac{2}{3} \cdot E_T]} \tag{4d}$$

is the positive scalar variable - Lagrange's coefficient, $\tilde{S}_{ij} = S_{ij} - \alpha_{ij}$ is the component of the reduced stress deviator $\tilde{\mathbf{D}}_\sigma$, $\tilde{C}(\varepsilon_{eq}^{(VP)}, \dot{\varepsilon}_{eq}^{(VP)}, T)$ is a materials parameter defining the components $\Delta\alpha_{ij}$ of the increment translation tensor $\Delta\mathbf{T}_\alpha$, $\varepsilon_{ij}^{(E)}$ is the cumulative elastic tensor component at time *t*, $E_T = \partial\sigma_Y(\varepsilon_{eq}^{(VP)}, \dot{\varepsilon}_{eq}^{(VP)}, T)/\partial\varepsilon_{eq}^{(VP)}$ is hardening modulus at the time *t*, $\dot{E}_T = \partial\sigma_Y(\varepsilon_{eq}^{(VP)}, \dot{\varepsilon}_{eq}^{(VP)}, T)/\partial\dot{\varepsilon}_{eq}^{(VP)}$ determines the sensitivity of the material at the rate of deformation, $\sigma_Y(\varepsilon_{eq}^{(VP)}, \dot{\varepsilon}_{eq}^{(VP)}, T)$ is thermodynamic yield stress of the material at time *t*.

Finally we obtain the isotropic material models which includes the combined effects of thermo-elasticity, termo-visco-plasticity for mixed hardening material and with a possibility of phase change to occur [39, 40]:

- **Increment components of visco-plastic strain tensor**:

$$\begin{aligned} \Delta\varepsilon_{ij}^{(VP)} &= \Delta\lambda \cdot \tilde{S}_{ij} = \\ &= \frac{\tilde{S}_{ij} \cdot C_{ijkl}^{(E)} \cdot \Delta\varepsilon_{kl} - \frac{2}{3} \cdot \sigma_Y(\varepsilon_{eq}^{(VP)}, \dot{\varepsilon}_{eq}^{(VP)}, T) \cdot \dot{E}_T \cdot \Delta\dot{\varepsilon}_{eq}^{(VP)}}{\tilde{S}_{ij} \cdot C_{ijkl}^{(TE)} \cdot \tilde{S}_{kl} + \frac{2}{3} \cdot [\sigma_Y(\varepsilon_{eq}^{(VP)}, \dot{\varepsilon}_{eq}^{(VP)}, T)]^2 \cdot [\tilde{C}(\varepsilon_{eq}^{(VP)}, \dot{\varepsilon}_{eq}^{(VP)}, T) + \frac{2}{3} \cdot E_T]} \cdot \tilde{S}_{ij} = \\ &= \tilde{S}_{ij}^{*} \cdot \tilde{S}_{kl} \cdot C_{klmn}^{(TE)} \cdot \Delta\varepsilon_{mn} - A \cdot \tilde{S}_{ij} = \tilde{S}^{**} \cdot \Delta\varepsilon_{ij} + \Delta\varepsilon_{ij}^{**}, \end{aligned} \tag{5}$$

  where the following substitute notation is used:

$$\tilde{S}^{**} = \tilde{S}_{ij}^{*} \cdot \tilde{S}_{mn} \cdot C_{ijmn}^{(E)}, \tag{5a}$$

$$\Delta\varepsilon_{ij}^{**} = -A \cdot \tilde{S}_{ij}^{*}, \tag{5b}$$

$$\tilde{S}_{ij}^{*} = \frac{\tilde{S}_{ij}}{\tilde{S}_{ij} \cdot C_{ijkl}^{(TE)} \cdot \tilde{S}_{kl} + \frac{2}{3} \cdot [\sigma_Y(\varepsilon_{eq}^{(VP)}, \dot{\varepsilon}_{eq}^{(VP)}, T)]^2 \cdot [\tilde{C}(\varepsilon_{eq}^{(VP)}, \dot{\varepsilon}_{eq}^{(VP)}, T) + \frac{2}{3} \cdot E_T]}, \tag{5c}$$

- **Increment components of total strain tensor:**

$$\Delta\varepsilon_{ij}=\frac{1}{1-{}_t^t\tilde{S}^{**}}\cdot\Bigg(D_{ijkl}^{(E)}\cdot\Delta\sigma_{kl}+ -\frac{\frac{2}{3}\cdot[\sigma_Y(\varepsilon_{eq}^{(VP)},\dot{\varepsilon}_{eq}^{(VP)},T)]\cdot\dot{E}_T\cdot\Delta\dot{\varepsilon}_z\cdot\tilde{S}_{ij}}{\tilde{S}_{ij}\cdot C_{ijkl}^{(E)}\cdot\tilde{S}_{kl}+\frac{2}{3}\cdot[\sigma_Y(\varepsilon_{eq}^{(VP)},\dot{\varepsilon}_{eq}^{(VP)},T)]^2\cdot\left(\tilde{C}(\varepsilon_{eq}^{(VP)},\dot{\varepsilon}_{eq}^{(VP)},T)+\frac{2}{3}\cdot E_T\right)}\Bigg), \tag{5d}$$

- **Increment components of total stress tensor:**

$$\begin{aligned}{}_t^\tau\Delta\sigma_{ij}={}_t^t\boldsymbol{C}_{ijkl}^{(TE)}\{{}_t^\tau\Delta\varepsilon_{kl}-\frac{{}_t^t\tilde{S}_{kl}}{{}_t^t\tilde{S}_{ij}\,{}_t^t\boldsymbol{C}_{ijkl}^{(TE)}\,{}_t^t\tilde{S}_{kl}+\frac{2}{3}{}_t^t\sigma_p^2({}_t^t\tilde{C}+\frac{2}{3}{}_t^tE_T)}\times\\ \times[{}_t^t\tilde{S}_{ij}\,{}_t^t\boldsymbol{C}_{ijkl}^{(TE)}({}_t^\tau\Delta\varepsilon_{kl}-{}_t^\tau\Delta\xi\delta_{kl}-{}_t^t\chi\,{}_t^\tau\Delta T\delta_{kl})+{}_t^t\tilde{S}_{ij}\,{}_t^\tau\Delta C_{ijkl}^{(TE)}\,{}_t^t\varepsilon_{kl}^{(E)}+\\ -\frac{2}{3}{}_t^t\sigma_p[\frac{\partial({}_t^t\sigma_p)}{\partial({}_t^t\dot{\varepsilon}_{eq})}{}_t^\tau\Delta\dot{\varepsilon}_{eq}+\frac{\partial({}_t^t\sigma_p)}{\partial({}_t^tT)}{}_t^\tau\Delta T]-{}_t^\tau\Delta\xi\delta_{kl}-{}_t^t\chi\,{}_t^\tau\Delta T\delta_{kl}]\}+\\ +{}_t^\tau\Delta C_{ijkl}^{(TE)}\,{}_t^t\varepsilon_{kl}^{(E)}\end{aligned} \tag{5e}$$

or:

$$\begin{aligned}\Delta\sigma_{ij}&=C_{ijkl}^{(TE)}(1-\tilde{S}^{**})\cdot\Delta\varepsilon_{kl}-C_{ijkl}^{(TE)}(\Delta\varepsilon_{kl}^{**}+\Delta\xi\cdot\delta_{kl}+\alpha_m\cdot\Delta T\cdot\delta_{kl})+\\ &+\Delta C_{ijkl}^{(TE)}\cdot\varepsilon_{kl}^{(E)}=C_{ijkl}^{(TE)*}\cdot\Delta\varepsilon_{kl}+\Delta\sigma_{ij}^{**},\end{aligned} \tag{5f}$$

where:

$$C_{ijkl}^{(TE)*}=C_{ijkl}^{(TE)}(1-\tilde{S}^{**}), \tag{5g}$$

$$C_{ijkl}^{(TE)}(T)=\lambda(T)\cdot\delta_{ij}\cdot\delta_{kl}+\mu(T)\cdot(\delta_{ik}\cdot\delta_{jl}+\delta_{il}\cdot\delta_{jk}) \tag{5h}$$

is the component of temperature dependent elastic constitutive tensor,

$$\Delta C_{ijkl}^{(TE)}(\Delta T)=\frac{\partial C_{ijkl}^{(TE)}(T)}{\partial T}\Delta T, \tag{5i}$$

is his increments,

$$\Delta\sigma_{ij}^{**}=-C_{ijkl}^{(TE)}(\Delta\varepsilon_{kl}^{**}+\Delta\xi\cdot\delta_{kl}+\alpha_m\cdot\Delta T\cdot\delta_{kl})+\Delta C_{ijkl}^{(TE)}\cdot\varepsilon_{kl}^{(E)}, \tag{5j}$$

is component of a increment stress tensor,

$$\tilde{S}^{**}=\tilde{S}_{ij}^{*}\cdot C_{ijmn}^{(TE)}\cdot\tilde{S}_{mn}, \tag{5k}$$

is positive scalar variable,

$$\Delta\varepsilon_{ij}^{**}=\tilde{S}_{ij}^{*}\cdot[-C_{ijmn}^{(TE)}\cdot\tilde{S}_{mn}(\alpha_m\cdot\Delta T+\Delta\xi)\cdot\delta_{ij}+\tilde{S}_{mn}\cdot\Delta C_{mnkl}^{(TE)}\cdot\varepsilon_{kl}^{(E)}-A], \tag{5l}$$

is component of a increment strain tensor,

$$\lambda(T)=\frac{E(T)\cdot\nu(T)}{[1+\nu(T)][1-2\nu(T)]},\qquad \mu(T)=\frac{E(T)}{2[1+\nu(T)]}, \tag{5m}$$

are Lame constants, while $E(T)$ and $\nu(T)$ are temperature-dependent Young's modulus and Poisson's ratio, respectively, δ_{ij} is the Kronecker delta, $\varepsilon_{kl}^{(E)}$ is accumulated components of elastic strain tensor at time *t*.

2.4. Model of contact tool-object

The qualification of the area real shape of the bodies' contact zones is combined with the determination in these areas of the states of loading mechanics (pressures and friction forces) and the state of the deformation of the object material, and the opposite. In practical considerations, these states are uncoupled in the way that the first one determines the shape and the field of the contact point area of bodies and then loads the result for these conditions. The above case of the contact problem has an essential meaning: the contact forces, contact stiffness, shape and field of the contact area of bodies, contact boundary conditions and friction conditions in this area. Model of contact tool-workpiece and its application in technological processes was presented in [28].

The incremental models (1)-(5) with model of contact tool-workpiece were used for practical engineering analysis. These models are used for variational formulation of non-linear equation of motion of the technological processes.

2.5. Mathematical incremental model of heat transfer

Using an updated Lagrange description, assuming knowledge of the temperature field in the initial moments t_0 and present time t, while looking for a solution to the next time $\tau = t + \Delta t$, where Δt is a very small incremental of time [12, 39]. Then the equation for a typical incremental step $t \to \tau$, in the global coordinate $\{\mathbf{z}\}$ is assumed:

$$div\{\lambda(T) \cdot grad[\Delta T(\mathbf{z}, \Delta t)]\} + \Delta q_{VI}[\cdot] + \Delta q_{VD}[\cdot] = C(T) \cdot \rho(T) \cdot \Delta \dot{T}(\mathbf{z}, \Delta t), \tag{6}$$

$$\Delta \dot{T}(\mathbf{z}, \Delta t) = \frac{\partial [\Delta T(\mathbf{z}, \Delta t)]}{\partial t} \tag{6a}$$

is the speed of incremental of the temperature, $\lambda(T)$, $C(T)$, $\rho(T)$ are depended on the temperature in the initial step: heat conductivity, heat capacity and mass density, however:

$$\begin{aligned} \Delta q_{VI}[\cdot] &= k_e \cdot \left[\frac{{}^{\tau}I^2 \cdot {}^{\tau}R({}^{\tau}T)}{{}^{\tau}V} - \frac{{}^{t}I^2 \cdot {}^{t}R({}^{t}T)}{{}^{t}V} \right] = \\ &= k_e \cdot \left[\left(\frac{{}^{\tau}I}{{}^{\tau}S_{\Sigma}} \right)^2 \cdot {}^{\tau}\rho_1({}^{\tau}T) - \left(\frac{{}^{t}I}{{}^{t}S_{\Sigma}} \right)^2 \cdot {}^{t}\rho_1({}^{t}T) \right], \end{aligned} \tag{6b}$$

$$\begin{aligned} \Delta q_{VD}[\cdot] &= \frac{(1-\xi) \cdot {}^{\tau}V}{t + \Delta t} \int_{{}^{t}_{t}\varepsilon_i^{(VP)}}^{{}^{\tau}_{\tau}\varepsilon_i^{(VP)}} {}^{\tau}_{\tau}\sigma_Y\left({}^{\tau}_{\tau}\varepsilon_{eq}^{(VP)}, {}^{\tau}_{\tau}\dot{\varepsilon}_{eq}^{(VP)}, {}^{\tau}T \right) + \\ &- \frac{(1-\xi) \cdot {}^{t}V}{t} \int_{{}^{t-\Delta t}_{t-\Delta t}\varepsilon_i^{(VP)}}^{{}^{t}_{t}\varepsilon_i^{(VP)}} {}^{t}_{t}\sigma_Y\left({}^{t}_{t}\varepsilon_{eq}^{(VP)}, {}^{t}_{t}\dot{\varepsilon}_{eq}^{(VP)}, {}^{t}T \right), \end{aligned} \tag{6c}$$

are the rate of incremental spatial heat sources generated by electrical current and by visco-plastic deformation, where $\sigma_Y(\varepsilon_{eq}^{(VP)}, \dot{\varepsilon}_{eq}^{(VP)}, T)$ is accumulated yield stress, depending on the history of visco-plastic strain $\varepsilon_{eq}^{(VP)}$ and strain rate $\dot{\varepsilon}_{eq}^{(VP)}$ and temperature T, $R(T)$ is temperature-dependent electrical resistance of material, $\rho_1(T)$ is temperature-dependent resistivity of material, S_{Σ} is the field of the areas contact Σ_k, $\xi = 0.05 \div 0.1$ is the coefficient energy absorption, k_e is the coefficient (for constant current k_e=1 and $k_e = 0.7 \div 0.97$ for alternating current).

The equation of heat transfer (6) ÷ (6c) are completed with the initial condition and the four boundary conditions.

Initial condition

Initial condition describes the temperature field at time which is the initial moment:

$$T(\mathbf{z}, t = t_0) = T_0(\mathbf{z}), \quad \mathbf{z} \in V. \tag{7}$$

In typical processing conditions in technological processes, the temperature of the object at time $t = t_0$ is constant, then:

$$T(\mathbf{z}, t = t_0) = T_0 = const \tag{8}$$

where T_0 is ambient temperature.

Boundary conditions

– ***conditions of I gender*** – the temperature may be prescribed at specific points in the surfaces, denoted by Σ_T, and/or at the specific points in the volume of the body, denoted by V_T:

$$T(\mathbf{z}, t) = T_o(\mathbf{z}, t), \quad \text{or} \quad \Delta T(\mathbf{z}, \Delta t) = \Delta T_o(\mathbf{z}, \Delta t), \quad \mathbf{z} \in \Sigma_T \tag{9}$$

– ***conditions of II gender*** – in the contact area tool and object Σ_k, heat flows:

$$-\quad \lambda_o(T)\,\mathbf{n}\circ grad\,[\Delta T_o(\mathbf{z},\Delta t)] = b_o(\Delta q_{FI} + \Delta q_{F\mu}),\ \ \mathbf{z}\in\Sigma_k, \tag{10}$$

$$-\quad \lambda_b(T)\,\mathbf{n}\circ grad\,[\Delta T_b(\mathbf{z},\Delta t)] = b_b(\Delta q_{FI} + \Delta q_{F\mu}),\ \ \mathbf{z}\in\Sigma_k, \tag{11}$$

– ***conditions of III gender*** (continuity of the heat flows):

$$-\quad \lambda_o(T)\mathbf{n}\circ grad[\Delta T_o(\mathbf{z},\Delta t)] = \frac{\Delta T_o(\mathbf{z},\Delta t) - \Delta T_b(\mathbf{z},\Delta t)}{R_s(\mathbf{z},\Delta t)} = -\lambda_b(T)\mathbf{n}\circ grad[\Delta T_b(\mathbf{z},\Delta t)],\ \ \mathbf{z}\in\sum\nolimits_k, \tag{12}$$

where R_s is the heat resistance in the surface contact (for ideal contact R_s=0), b_o and b_b is the heat division coefficients for burnishing element (b) and object (o), $\mathbf{n}\circ\mathrm{grad}[\Delta T(\cdot)]$ is the scalar product, $\Delta q_{SI}[\cdot]$ and $\Delta q_{S\mu}[\cdot]$ are the rate of incremental surface heat sources generated by electrical current (heat of Joule's) and fretting per unit surface,

– ***conditions of IV gender*** – they are in areas Σ_C i Σ_R, in which exchange heat is on road convection and radiation, then the boundary conditions are defined by:

$$\Delta q_C = \alpha_C(T)\cdot\Delta T = -\lambda(T)\mathbf{n}\circ grad[\Delta T(\mathbf{z},\Delta t)],\quad \mathbf{z}\in\Sigma_c \tag{13}$$

$$\Delta q_R = \alpha_R(T)\cdot\Delta T = -\lambda(T)\mathbf{n}\circ grad[\Delta T(\mathbf{z},\Delta t)],\quad \mathbf{z}\in\Sigma_R \tag{14}$$

where Δq_C and Δq_R are incremental intensity flow heat exchange with the environment by convection and radiation, $\alpha_C(T)$ and $\alpha_R(T)$ are temperature - dependent convection coefficient and radiation coefficient [3].

Equations (6)-(6c) with initial condition (7) and (8), and boundary conditions (9)÷(14) are a full mathematical description of heat transfer during the technological processes, at the typical incremental time step. The analytical solution is impossible, therefore in the next section we are introduced variational formulation.

3. VARIATIONAL FORMULATION

3.1. Variational equation of motion and deformation

The equation of motion and deformation of the object is developed in the updated Lagrange's formulation. At this case a functional increment is formulated for increment displacement $\Delta F(\Delta\ddot{u}_i,\Delta\dot{u}_i,\Delta u_i) = \Delta F(\cdot)$, where $\Delta\ddot{u}_i$ are the i*th* increment components of the acceleration vector. Using the conditions of stationary of functional $\Delta F(\cdot)$, we obtain a variational equation of motion and deformation:

$$\begin{aligned}
\delta[\Delta\mathbf{F}(\cdot)] &= \int_V \rho\cdot(\ddot{u}_i + \Delta\ddot{u}_i)\cdot\delta(\Delta u_i)\cdot dV + \alpha_1\cdot\int_V \rho\cdot\Delta\dot{u}_i\cdot\delta(\Delta u_i)\cdot dV + \\
&-2\omega\cdot\int_V \rho\cdot\Delta\dot{u}_i\cdot\Omega_{ij}\cdot\delta(\Delta u_j)\cdot dV + \frac{1}{2}\cdot\alpha_2\cdot\int_V \Delta\dot{\tilde{\varepsilon}}_{ij}\cdot C^{(E)}_{ijkl}\cdot\delta(\Delta\tilde{\varepsilon}_{kl})\cdot dV + \\
&+\frac{1}{2}\cdot\alpha_2\cdot\int_V \Delta\dot{\tilde{\varepsilon}}_{ij}\cdot C^{(E)}_{ijkl}\cdot\delta(\Delta\bar{\varepsilon}_{kl})\cdot dV + \frac{1}{2}\cdot\alpha_2\cdot\int_V \Delta\dot{\bar{\varepsilon}}_{ij}\cdot C^{(E)}_{ijkl}\cdot\delta(\Delta\tilde{\varepsilon}_{kl})\cdot dV + \\
&+\frac{1}{2}\cdot\alpha_2\cdot\int_V \Delta\dot{\bar{\varepsilon}}_{ij}\cdot C^{(E)}_{ijkl}\cdot\delta(\Delta\bar{\varepsilon}_{kl})\cdot dV + \frac{1}{2}\cdot\alpha_2\cdot\int_V \delta(\Delta\dot{\tilde{\varepsilon}}_{kl})\cdot C^{(E)}_{ijkl}\cdot\Delta\tilde{\varepsilon}_{kl}\cdot dV + \\
&+\frac{1}{2}\cdot\alpha_2\cdot\int_V \Delta\dot{\bar{\varepsilon}}_{ij}\cdot C^{(E)}_{ijkl}\cdot\delta(\Delta\bar{\varepsilon}_{kl})\cdot dV + \frac{1}{2}\cdot\alpha_2\cdot\int_V \delta(\Delta\dot{\tilde{\varepsilon}}_{kl})\cdot C^{(E)}_{ijkl}\cdot\Delta\tilde{\varepsilon}_{kl}\cdot dV + \\
&+\frac{1}{2}\cdot\alpha_2\cdot\int_V \delta(\Delta\dot{\tilde{\varepsilon}}_{kl})\cdot C^{(E)}_{ijkl}\cdot\Delta\bar{\varepsilon}_{kl}\cdot dV + \frac{1}{2}\cdot\alpha_2\cdot\int_V \delta(\Delta\dot{\bar{\varepsilon}}_{kl})\cdot C^{(E)}_{ijkl}\cdot\Delta\tilde{\varepsilon}_{kl}\cdot dV + \\
&+\frac{1}{2}\cdot\alpha_2\cdot\int_V \delta(\Delta\dot{\bar{\varepsilon}}_{kl})\cdot C^{(E)}_{ijkl}\cdot\delta(\Delta\bar{\varepsilon}_{kl})\cdot dV + \int_V \Delta\tilde{\varepsilon}_{ij}\cdot C^{(E)*}_{ijkl}\cdot\delta(\Delta\tilde{\varepsilon}_{kl})\cdot dV +
\end{aligned} \tag{15}$$

$$+\int_V \Delta\tilde{\varepsilon}_{ij}\cdot C_{ijkl}^{(E)*}\cdot\delta(\Delta\bar{\varepsilon}_{kl})\cdot dV+\int_V \Delta\bar{\varepsilon}_{ij}\cdot C_{ijkl}^{(E)*}\cdot\delta(\Delta\tilde{\varepsilon}_{kl})\cdot dV+$$

$$+\int_V \Delta\bar{\varepsilon}_{ij}\cdot C_{ijkl}^{(E)*}\cdot\delta(\Delta\bar{\varepsilon}_{kl})\cdot dV+\frac{1}{2}\cdot\int_V (T_{ij}+\Delta\sigma_{ij}^{**})\cdot\delta(\Delta\tilde{\varepsilon}_{kl})\cdot dV+$$

$$+\frac{1}{2}\cdot\int_V (T_{ij}+\Delta\sigma_{ij}^{**})\cdot\delta(\Delta\bar{\varepsilon}_{kl})\cdot dV-\omega^2\cdot\int_V \rho\cdot r_i\cdot\Omega_{ij}\cdot\Omega_{ij}\cdot\delta(\Delta u_i)\cdot dV+$$

$$-\int_V \rho\cdot(f_i+\Delta f_i)\cdot\delta(\Delta u_i)\cdot dV-\int_{\Sigma_k}(\hat{q}_i+\Delta\hat{q}_i)\cdot\delta(\Delta u_i)\cdot d\Sigma_k=0,$$

where T_{ij} are the components of Cauchy's stress tensor, $\Delta\dot{\bar{\varepsilon}}_{ij}$, $\Delta\dot{\tilde{\varepsilon}}_{ij}$ are linear and non-linear increment components of Green-Lagrange's strain rate tensor, $\Delta\bar{\varepsilon}_{ij}=(\Delta u_{i,j}+\Delta u_{j,i})/2$ and $\Delta\tilde{\varepsilon}_{ij}=(\Delta u_{i,k}\cdot\Delta u_{j,k})/2$ are the linear and non-linear increments components of Green-Lagrange's strain tensor, respectively, ρ is the mass density at time *t*, ε_{ij} are a accumulated components of total strain tensor at time *t* (depend on the history of deformation), f_i, Δf_i are the components of the internal force and incremental force vectors, respectively, q_i, Δq_i are the components of the externally applied surface force and surface incremental force vectors in the contact body zones, respectively, Ω_{ij} is the component of the gyro tensor. The integrations are performed over the volume *V* and surface Σ of the body, respectively.

3.2. Variational equation of heat transfer

For the variational formulation of the equation of heat transfer in the technological processes, at the typical time step, is introduced an incremental functional $\Delta\mathbf{F}(\Delta\dot{T},\ \Delta T',\ \Delta T,\ldots)$, in which is one independent field – it is temperature field, and its derivatives: $\Delta\dot{T}=d(\Delta T)/dt$, $\Delta T'=d(\Delta T)/dy_3$. This functional has differential equations (6)-(6c) in the global Cartesians coordinate {**z**} and boundary conditions (9)÷(14). Using the conditions of stationarity of functional we obtain (because ΔT is the only variable) in the global system {**z**} [39]:

$$\delta[\Delta\dot{T},\Delta T',\Delta T]=\int_V\left[\sum_{i=1}^{3}\lambda_i(T)\cdot\frac{\partial(\Delta T)}{\partial z_i}\cdot\delta\left(\frac{\partial(\Delta T)}{\partial z_i}\right)\right]\cdot dV+$$
$$+\int_V\frac{\partial(\Delta T)}{\partial t}\cdot C(T)\cdot\rho(T)\cdot\delta(\Delta T)\cdot dV+\int_V\delta\left(\frac{\partial(\Delta T)}{\partial t}\right)\cdot C(T)\cdot\rho(T)\cdot\Delta T\cdot dV+$$
$$-\int_V\Delta q_{VI}[\cdot]\cdot\delta(\Delta T)\cdot dV-\int_V\Delta q_{VO}[\cdot]\cdot\delta(\Delta T)\cdot dV-\int_{\Sigma_k}b\cdot\Delta q_{FI}[\cdot]\cdot\delta(\Delta T)\cdot d\Sigma_k+\tag{16}$$
$$-\int_{\Sigma_k}b\cdot\Delta q_{F\mu}[\cdot]\cdot\delta(\Delta T)\cdot d\Sigma_k+\int_{\Sigma_k}\frac{\Delta T_o-\Delta T_b}{2R_s}\cdot\delta(\Delta T)\cdot d\Sigma_k+$$
$$+\int_{\Sigma_C}\alpha_C(T)\cdot\delta(\Delta T)\cdot d\Sigma_C+\int_{\Sigma_R}\alpha_R(T)\cdot\delta(\Delta T)\cdot d\Sigma_R-\int_{\Sigma_T}\Delta T\cdot\delta(\Delta T)\cdot d\Sigma_T=0.$$

Equation (16) is variational formulation of heat transfer at the typical step time, in updated Lagrange's description in technological processes. The equations (15) and (16) provides the basis for the finite element discretization for obtain the solution.

4. IMPLEMENTATION OF THE FINITE ELEMENT METHOD

4.1. Discretized equation of motion

Assume that the complete body under consideration has been idealized as an assemblage of finite elements, we obtain the discretized equation of motion for an assemblage of elements in the global coordinate {**z**}, at typical step time $t\to\tau=t+\Delta t$, in the form:

$$\mathbf{M}\cdot\Delta\ddot{\mathbf{r}}+\mathbf{C}\cdot\Delta\dot{\mathbf{r}}+(\mathbf{K}+\Delta\mathbf{K})\cdot\Delta\mathbf{r}=\Delta\mathbf{R}+\Delta\mathbf{F}+\mathbf{R}+\mathbf{F},\tag{17}$$

where the mass matrix **M**, damping matrix **C** stiffness matrix **K** and force vector **F** are knows at time *t*, however the increment stiffness matrix Δ**K**, external incremental load vector Δ**R**, internal incremental forces vector Δ**F**, and the incremental vectors of displacement $\Delta\mathbf{r}$, velocity $\Delta\dot{\mathbf{r}}$, and acceleration $\Delta\ddot{\mathbf{r}}$ of finite element assemblage at typical step time are not knows. For solve of this problem the DEM and DIM integration methods are used.

4.2. Discretized equation of heat transfer

Assume that the complete body under consideration has been idealised as an assemblage of finite elements, we have, at step time $t \to t+\Delta t$, for element *e* and *m*:

$$\begin{aligned}
&\Delta T^{(e)}(\cdot) = [\mathbf{H}^{(e)}(\cdot)]\cdot\{\Delta\mathbf{\Theta}^{(e)}\},\\
&\Delta T'^{(e)}(\cdot) = [\mathbf{B}^{(e)}(\cdot)]\cdot\{\Delta\mathbf{\Theta}^{(e)}\},\\
&\Delta T'^{(e)}(\cdot) = [\mathbf{B}_3{}^{(e)}(\cdot)]\cdot\{\Delta\mathbf{\Theta}^{(e)}\},\\
&\Delta T^{(m)}(\cdot) = [\mathbf{H}^{S(m)}(\cdot)]\cdot\{\Delta\mathbf{\Theta}^{(m)}\},\\
&\Delta \dot{T}^{(e)}(\cdot) = [\mathbf{B}^{(e)}(\cdot)]\cdot\{\Delta\dot{\mathbf{\Theta}}^{(e)}\},
\end{aligned} \tag{18}$$

where: $\Delta T^{(e)}$ is the temperature increment of finite element *e*, $\{\Delta\mathbf{\Theta}^{(e)}\}$ and $\{\Delta\dot{\mathbf{\Theta}}^{(e)}\}$ are vectors of increments in the nodal point temperature and of increments in the nodal point temperature rate, at all *N* nodal points, respectively.

Using the relation (18) in the variational equation (16), we obtain the discretized equation of heat transfer equilibrium in the global coordinate $\{\mathbf{z}\}$ (the non stabilized heat transfer):

$$[\mathbf{C}]\{\Delta\dot{\mathbf{\Theta}}\} + ([\mathbf{K}^K] + [\mathbf{K}^C] + [\mathbf{K}^R] + [\mathbf{K}^{IV}])\{\Delta\mathbf{\Theta}\} = \{\Delta\mathbf{Q}\} + \{\Delta\mathbf{Q}^{\mathrm{I}}\}, \tag{19}$$

where $[\mathbf{C}]$ and $[\mathbf{K}^{\mathrm{K}}]$, $[\mathbf{K}^{\mathrm{C}}]$, $[\mathbf{K}^{\mathrm{R}}]$, $[\mathbf{K}^{\mathrm{IV}}]$ are the heat capacities, conductivity, convection and radiation matrices and total nodal point conditions of IV gender, $\{\Delta\mathbf{Q}\}$ is the nodal point increment heat flow input vector, $\{\Delta\mathbf{Q}^{\mathrm{I}}\}$ is the vector of nodal point of the boundary conditions of I gender.

5. DYNAMIC EXPLICIT METHOD ALGORITHMS

5.1. Solution the discretized equation of motion

Assuming that the temporary step time Δt is very small, it is possible to remove the incremental stiffness matrix $(\Delta\mathbf{K} \approx 0)$ and internal incremental force vector $(\Delta\mathbf{F} \approx 0)$. Then, using the principle of incremental decomposition, approximating the $\dot{\mathbf{r}}$ and $\ddot{\mathbf{r}}$ in terms of $\mathbf{r}$ in equation (17) using the central difference method (DEM), and using the following approximate [11]:

$${}^{t}\dot{\mathbf{r}} = \frac{1}{2\Delta t}\cdot\left({}^{\tau}\mathbf{r} - {}^{t-\Delta t}\mathbf{r}\right), \qquad {}^{t}\ddot{\mathbf{r}} = \frac{1}{\Delta t^2}\cdot\left({}^{\tau}\mathbf{r} - 2\cdot{}^{t}\mathbf{r} + {}^{t-\Delta t}\mathbf{r}\right), \tag{20}$$

we obtain the solution of ${}^{\tau}_{t}\mathbf{r}$:

$$\tilde{\mathbf{M}}\cdot{}^{\tau}_{t}\mathbf{r} = \tilde{\mathbf{Q}}, \tag{21}$$

where $\tilde{\mathbf{M}}$ is the effective mass matrix and $\tilde{\mathbf{Q}}$ the effective load vector:

$$\tilde{\mathbf{M}} = a_0\cdot\mathbf{M} + a_1\cdot\mathbf{C} \tag{21a}$$

$$\tilde{\mathbf{Q}} = \mathbf{F} + \mathbf{R} + a_0\cdot\mathbf{M}\cdot\left(2\cdot{}^{t}\mathbf{r} - {}^{t-\Delta t}\mathbf{r}\right) + a_1\cdot\mathbf{C}\cdot{}^{t-\Delta t}\mathbf{r}, \tag{21b}$$

with the integration constants: $a_0 = 1/\Delta t^2$, $a_1 = 1/(2\Delta t)$.

Step-by-step solution using the Central Difference Method

In this section, the Central Difference Method [79-81] is adopted to solve Eq. (21)-(21b) with initial and boundary conditions.

Initial calculations:

1. Form mass $\mathbf{M}$ and damping $\mathbf{C}$ matrices.
2. Initialise vectors: ${}^{0}\mathbf{r}$, ${}^{0}\dot{\mathbf{r}}$ and ${}^{0}\ddot{\mathbf{r}}$.
3. Select a time step $\Delta t < \Delta t_{cr} = T_N/\pi$ and calculate the integration constants a_0 and a_1.

4. Calculate vector ${}^{-\Delta t}\mathbf{r}$.

5. Form an effective stiffness matrix $\tilde{\mathbf{M}}$ from equation (21a).

For each time step:

1. Calculate the effective load vector $\tilde{\mathbf{Q}}$ from equation (21b).
2. Partitioning the equilibrium equation for two blocks, write the problem in the form:

$$\begin{bmatrix} \tilde{\mathbf{M}}_{11}^{n\times n} & \tilde{\mathbf{M}}_{12}^{n\times w} \\ \tilde{\mathbf{M}}_{21}^{w\times n} & \tilde{\mathbf{M}}_{22}^{w\times w} \end{bmatrix} \begin{Bmatrix} {}_t^{\tau}\mathbf{r}_1^{n\times 1} \\ {}_t^{\tau}\mathbf{r}_2^{w\times 1} \end{Bmatrix} = \begin{Bmatrix} \tilde{\mathbf{Q}}_1^{n\times 1} \\ \tilde{\mathbf{Q}}_2^{w\times 1} \end{Bmatrix},$$

where vectors $\mathbf{r}_2^{w\times 1}$, $\tilde{\mathbf{Q}}_1^{n\times 1}$ are known and vectors $\mathbf{r}_1^{n\times 1}$, $\tilde{\mathbf{Q}}_2^{w\times 1}$ are unknown.

3. Solve for the displacement vector ${}_t^{\tau}\mathbf{r}_1^{n\times 1}$:

$${}_t^{\tau}\mathbf{r}_1^{n\times 1} = (\tilde{\mathbf{M}}_{11}^{n\times n})^{-1} \cdot [\tilde{\mathbf{Q}}_1 - \tilde{\mathbf{M}}_{12}^{n\times w} \cdot {}_t^{\tau}\mathbf{r}_2^{w\times 1}],$$

4. Substitute vector ${}_t^{\tau}\mathbf{r}_1^{n\times 1}$ into the equation:

$$\tilde{\mathbf{Q}}_2^{w\times 1} = \tilde{\mathbf{M}}_{21}^{w\times n} \cdot {}_t^{\tau}\mathbf{r}_1^{n\times 1} + \tilde{\mathbf{M}}_{22}^{w\times w} \cdot {}_t^{\tau}\mathbf{r}_2^{w\times 1},$$

and solve to obtain the load vector $\tilde{\mathbf{Q}}_2^{w\times 1}$ in the tool-object contact zone.

5. Calculate the vectors ${}^{t}\dot{\mathbf{r}}$ and ${}^{t}\ddot{\mathbf{r}}$ from equation (20).

5.2. Solution the discretized equation of heat transfer

Application the Dynamic Implicit Method (DIM) to solve the discretized equation of heat transfer was presented in [12, 39]. In this section to solve this equation the Dynamic Explicit Method (DEM) was presented. Using the principle of incremental decomposition, approximating the ${}^{t}\dot{\boldsymbol{\theta}}$ in terms of $\boldsymbol{\theta}$ in equation (19) using the central difference method (DEM), and using the following approximation:

$$\{{}^{t}\dot{\boldsymbol{\theta}}\} = \frac{1}{2\Delta t} \cdot (\{{}^{\tau}\boldsymbol{\theta}\} - \{{}^{t-\Delta t}\boldsymbol{\theta}\}), \tag{22}$$

we obtain the solution of $\{{}^{\tau}\boldsymbol{\theta}\}$:

$$[\mathbf{C}] \cdot \{{}^{\tau}\boldsymbol{\theta}\} = \{\tilde{\mathbf{Q}}\}, \tag{23}$$

where $\{\tilde{\mathbf{Q}}\}$ the effective load vector:

$$\{\tilde{\mathbf{Q}}\} = \{\Delta\mathbf{Q}\} + \{\Delta\mathbf{Q}^{\mathrm{I}}\} + [\mathbf{C}]\frac{1}{2\Delta t} \cdot \{{}^{t-\Delta t}\boldsymbol{\theta}\} + [\mathbf{C}]\frac{1}{2\Delta t} \cdot \{{}^{t-\Delta t}\dot{\boldsymbol{\Theta}}\} - [\tilde{\mathbf{K}}]\{{}^{t}\Delta\boldsymbol{\Theta}\}. \tag{23a}$$

Step-by-step solution using the Central Difference Method

In this section, the Central Difference Method [79-81] is adopted to solve Eqs. (22) and (22a).

Initial calculations:

1. Form matrix $[{}^{t}\mathbf{C}]$, $[{}^{t}\mathbf{K}^{k}]$, $[{}^{t}\mathbf{K}^{c}]$, $[{}^{t}\mathbf{K}^{r}]$ and $[{}^{t}\mathbf{K}^{\mathrm{IV}}]$ and calculation the effective matrix $[{}^{t}\tilde{\mathbf{K}}]$:

$$[{}^{t}\tilde{\mathbf{K}}] = [{}^{t}\mathbf{C}] + [{}^{t}\mathbf{K}^{k}] + [{}^{t}\mathbf{K}^{c}] + [{}^{t}\mathbf{K}^{r}] + [{}^{t}\mathbf{K}^{\mathrm{IV}}]$$

2. Form vectors $\{\Delta\mathbf{Q}\}$ and $\{\Delta\mathbf{Q}^{\mathrm{I}}\}$.
3. Calculate (initialise) $\{{}^{t-\Delta t}\boldsymbol{\theta}\}$, $\{{}^{t-\Delta t}\dot{\boldsymbol{\Theta}}\}$ and $\{{}^{t}\Delta\boldsymbol{\Theta}\}$.

For each time step:

1. Calculate the effective load vector $\tilde{\mathbf{Q}}$ from equation (23a).
2. Partitioning the equilibrium equation for two blocks, write the problem in the form:

$$\begin{bmatrix} \mathbf{C}_{11}^{n\times n} & \mathbf{C}_{12}^{n\times w} \\ \mathbf{C}_{21}^{w\times n} & \mathbf{C}_{22}^{w\times w} \end{bmatrix} \begin{Bmatrix} {}^{\tau}\boldsymbol{\theta}_1^{n\times 1} \\ {}^{\tau}\boldsymbol{\theta}_2^{w\times 1} \end{Bmatrix} = \begin{Bmatrix} \tilde{\mathbf{Q}}_1^{n\times 1} \\ \tilde{\mathbf{Q}}_2^{w\times 1} \end{Bmatrix},$$

where vectors $\boldsymbol{\theta}_2^{w\times 1}$, $\tilde{\mathbf{Q}}_1^{n\times 1}$ are known and vectors $\boldsymbol{\theta}_1^{n\times 1}$, $\tilde{\mathbf{Q}}_2^{w\times 1}$ are unknown.

3. Solve for the displacement vector ${}^{\tau}_{t}\boldsymbol{\theta}_1^{n\times 1}$:

$${}^{\tau}\boldsymbol{\theta}_1^{n\times 1} = (\mathbf{C}_{11}^{n\times n})^{-1} \cdot [\tilde{\mathbf{Q}}_1 - \mathbf{C}_{12}^{n\times w} \cdot {}^{\tau}\boldsymbol{\theta}_2^{w\times 1}],$$

4. Substitute vector ${}^{\tau}\boldsymbol{\theta}_1^{n\times 1}$ into the equation:

$$\tilde{\mathbf{Q}}_2^{w\times 1} = \mathbf{C}_{21}^{w\times n} \cdot {}^{\tau}\boldsymbol{\theta}_1^{n\times 1} + \mathbf{C}_{22}^{w\times w} \cdot {}^{\tau}\boldsymbol{\theta}_2^{w\times 1},$$

and solve to obtain the load vector $\tilde{\mathbf{Q}}_2^{w\times 1}$ in the tool-object contact zone.

5. Calculate the vectors ${}^{t}\dot{\boldsymbol{\theta}}$ from equation (22).

6. EXAMPLES OF NUMERICAL SOLUTION

6.1. Burnishing rolling process with electrical current [3]

The analysis has been carried out using the following data: type of part - a roller, diameter of roller $d = 30$ mm; roughness profile of the transverse surface in accordance with projection case I (triangular asperities) with the parameters $R_t = 0.142$ mm; $\alpha_1 = \alpha_2 = 55^\circ$; $p_t = 0.2$ rpm; burnishing by means of a $D = 60$ mm diameter roller-shaped element; depth of burnishing $g = 0.071$ mm; burnishing feed $p_b = p_t = 0.2$ rpm; velocity of burnishing rolling $v_b = 1.5$ m·s^{-1}. Also, we assumed the data:

– intensity of electrical current: $I = 0; 100; 300; 500; 700,$ A,
– heat capacity: $C = 484 + 0.01 \cdot \Delta T$, J/(kg·K),
– resistivity:

$$\rho_{1o} = 15 \cdot (1 + 0.00196 \cdot \Delta T) \cdot 10^{-8}, \ \Omega\text{m, (object)},$$

– coefficient of fretting:

$$\mu = \mu_0 \cdot (1 - 0.003 \cdot v_r) \cdot (1 - 0.000015 \cdot \Delta T),$$

– heat conductivity coefficients:

$$\lambda_o = 42 - 0.012 \cdot \Delta T, \ \text{W/(m·K), (object)},$$

$$\lambda_b = 13.2207 - 0.0032 \cdot \Delta T, \ \text{W/(m·K), (tool)},$$

– mass density: $\rho = 7850 / (1 + \alpha \cdot \Delta T)$, kg·m^{-3}.

We demonstrate the results of non-linear 3D analysis in figures 3÷5.

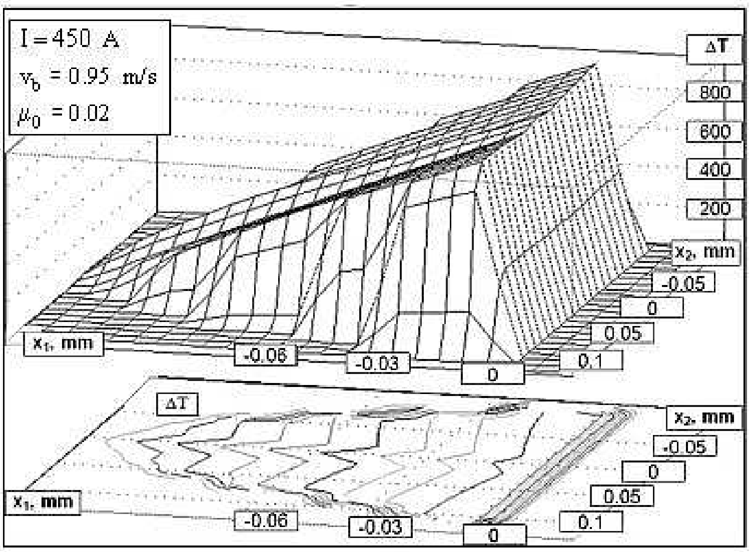

Fig. 3. The field of resultant temperature increment ΔT on surface in contact with the tool

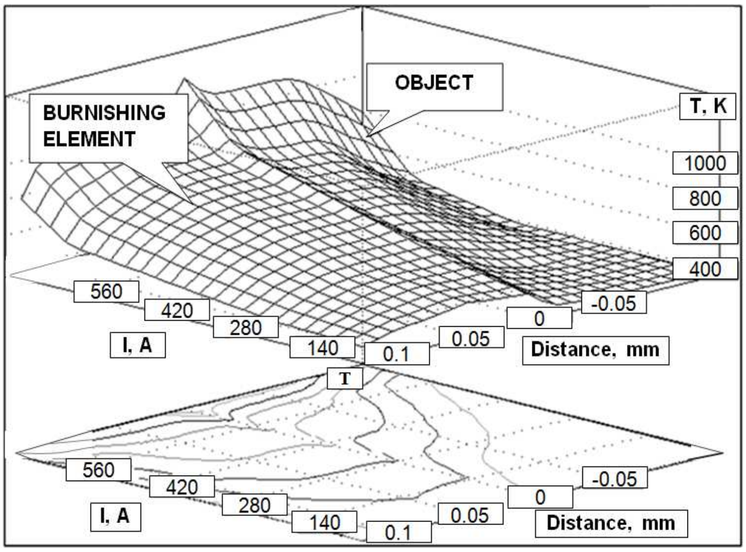

Fig. 4. *Distribution of the resultant temperature T into surface layer object and tool on axis* $x_3(x_1 = x_2 = 0)$, *depending on the intensity of the electric current for* $v_b = 1.5\ m{\cdot}s^{-1}$ *and* $\mu_0 = 0.02$ *(perfect contact* $R_s = 0$*)*

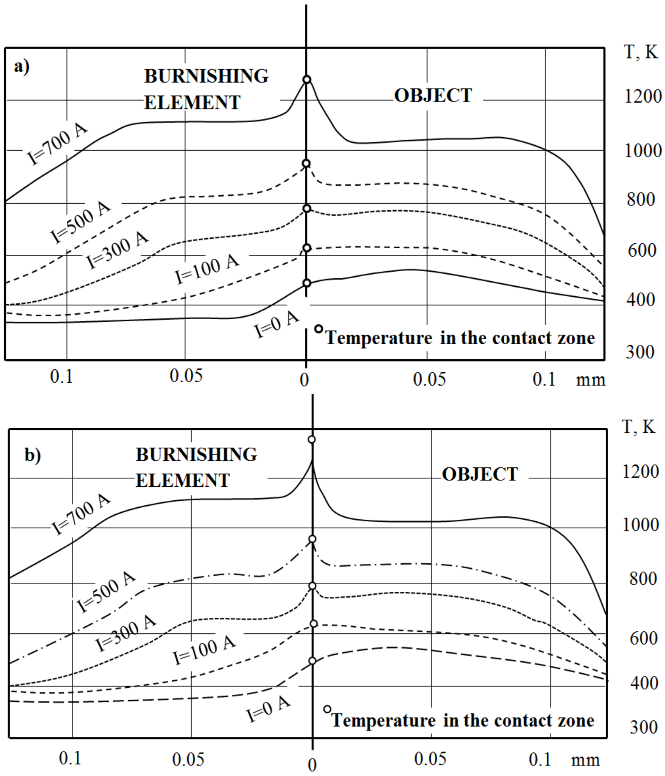

Fig. 5. *Temperature distribution in the tool and object in the axial section for the perfect contact* $R_s = 0$ *(a) and with thermal resistance* $R_s = 0.094\ m^2{\cdot}K{\cdot}W^{-1}$, *(the condition IV) at the contact tool-object) (b)*

In order to verification of results of computer analysis experimental research of the process of burnishing with current were conducted in stand shown in figure 6.

Figure 7 shows scanning micrographs of exemplary microstructures of samples before and after burnishing.

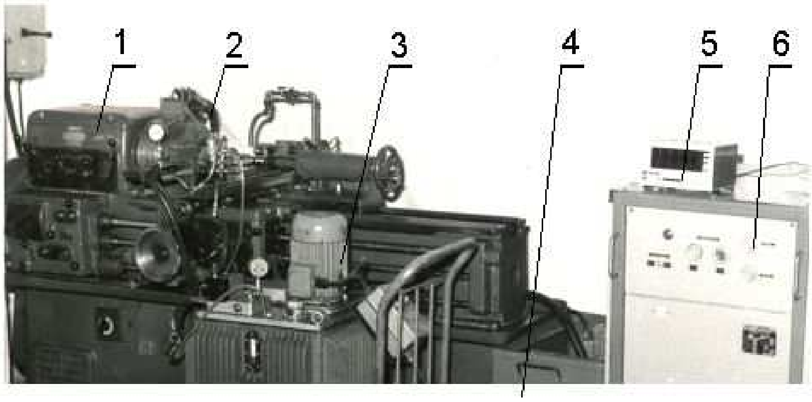

Fig. 6. *Stand for burnishing rolling with current [3]: 1 – lathe, 2 – burnishing attachment, 3 – hydraulic feeder, 4 – coolant feeder, 5 – ammeter, 6 – welding transformer*

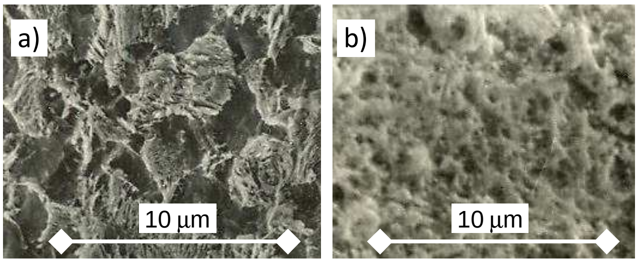

Fig. 7. *Exemplary microstructures of surface layer before burnishing (a) (initial pearlitic - ferritic microstructure for steel C55) and after roller burnishing with current (b) (martensitic micro-structure) [3]*

6.2. Thread rolling process [26]

Simulation studies the rolling process of the thread (Fig. 8) was carried out in two stages. In the first stage, using a sensitivity analysis the effective discrete model of the process was determined. In a second step, using the discrete model developed, the calculations were performed in order to define the influence of friction coefficient on the state of deformation (displacements and strain) and stress in the surface layer of the object. The rolling process were considered as isothermal, carried out cold at ambient temperature.

The numerical analysis for 2D states of deformation and 3D states of stress was applied on the example of steel C55. The tool is considered as rigid $E \to \infty$ or elastic body, however the material model as an elasto/visco-plastic body with non-linear hardening. The model has discretized by finite element PLANE183 with non-linear function of the shape.

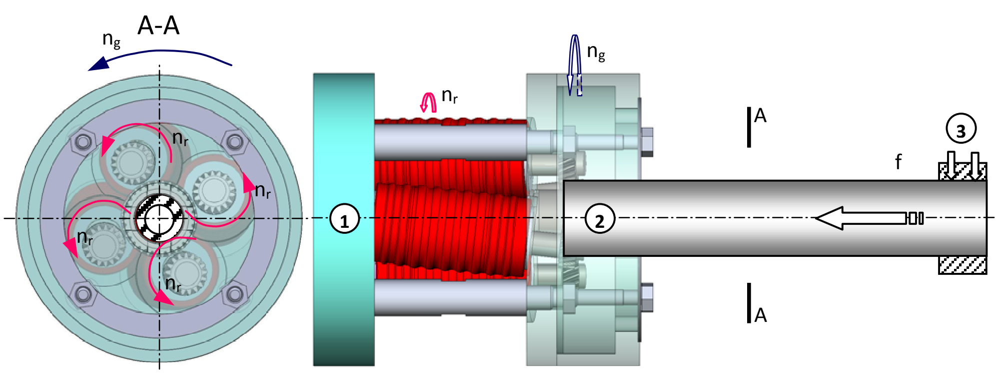

Fig. 8. *Computer model of the axial thread rolling process on cold of the thread on the bars or pipes by an angle head comprising four rollers [26]: 1 – head, 2 – blank, 3 – handle*

6.2.1. Sensitivity analysis

The sensitivity analysis is defined as a measure of the response of the system changes due to a change of the selected parameter called the decision variable. In the case of the FEM analysis of the thread rolling process, an important issue is to determine how is the sensitivity of the maximum strain and stress at points of discrete body to: changing the size of the finite element, number of finite elements and element shape function.

Influence of the size of the finite element

The shape factor SF of the finite element is defined as the ratio of height A to width B of the finite element ($SF = B/A$) (Fig. 9).

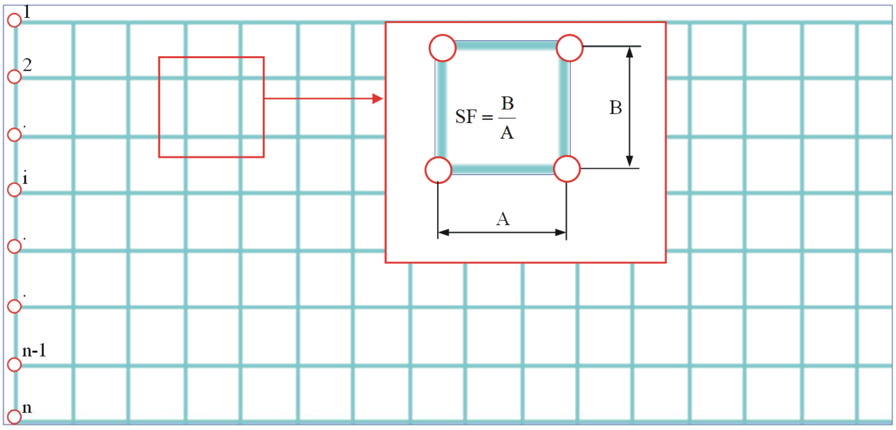

Fig. 9. *Finite element mesh, the distribution of successive layers and the definition of shape factor*

It is preferred that the shape factor was close to unity. Due to the a strong geometrical non-linearity, particularly in the bottom and top of the thread, the models were used, from discrete finite elements with a big shape factor. In order to reduce the number of degrees of freedom of the model is to minimize the number of *FE* by increasing the height of elements. In order to determine the rational of the shape of *FE* was performed computer simulations to determine the influence of the *SF* on the distribution of stress and strain and the accuracy of the mapping thread profile. Due to the symmetry of the model examined half of the profile. The analysis was performed using an application developed in ANSYS system. For the discretization of the object element type PLANE183 was used with eight key 8-node with a non-linear shape function. In order to determine the maximum of the equivalent stress and strain by the hypothesis Huber-Mises-Hencky in the thread, depending on the shape factor *SF* variants of models were developed with different mesh division. Table 1 summarizes the computational variants of the thread. The following values of the shape factor was considered: $SF = 0{,}11;\ 0{,}25;\ 0{,}43;\ 0{,}66,\ 1;\ 1{,}5;\ 2{,}33;\ 4\ i\ 9$.

Tab. 1. Variants of the finite element mesh

SF	**0,11**	**0,25**	**0,43**	**0,66**	**1**	**1,5**	**2,33**	**4**	**9**
n – number of layers	205	182	160	136	114	91	91	46	23
NFE – number of FE	8352	14834	19484	22048	23054	22220	19546	15032	8678
NN – number of nodes	25645	44931	58697	66221	69067	66393	58199	44485	25251
NDF – number degrees of freedom	51290	89862	117394	132442	138134	132786	116398	88970	51042

Examples of simulation results influence of the *SF* on the accuracy the mapping tool, shown in Figure 10. The red line indicates outline tool. From the drawings it is apparent that the correct image on the contour of the tool takes place only for $SF \geq 1$. For the $SF \leq 0{,}11$ following was observed finite element object penetration by the elements of the tool. In Figure 7.4 shows the effect of *SF* on the states of maximum equivalent stress and strain. Most beneficial results calculated stress and strain are obtained for $SF = 0{,}67 \div 1{,}5$. Further increase *SF* (up to nine) does not have a significant impact on the accuracy of the calculation, defined as the difference values in the elements and nodes.

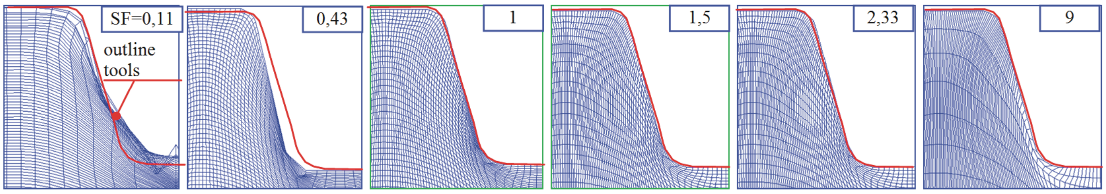

Fig. 10. View of deformation of the finite element mesh for different shape factor [26]

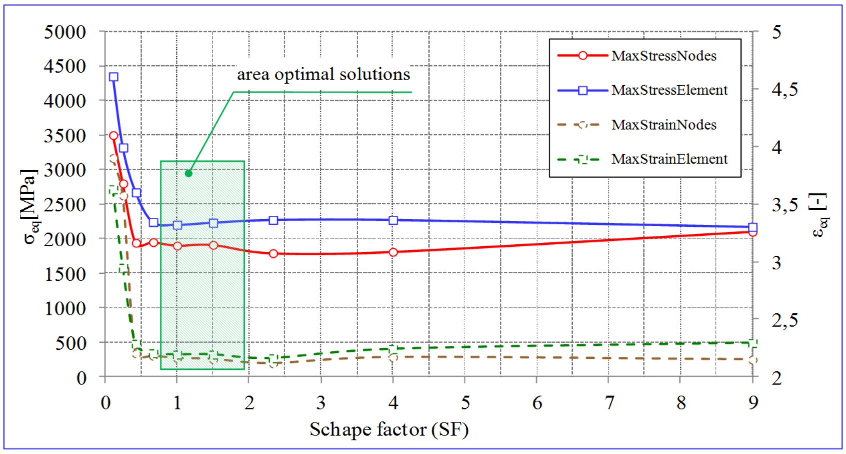

Fig. 11. The calculated maximum equivalent stress and strain values for different values of shape factor finite element [26]

The calculation results presented in Figure 11 demonstrate a strong convergence with the values of shape factor. In the range of aspect ratio, it was found that the best solutions were obtained with $SF = 0,67 \div 1,5$. Consequently, in the subsequent analyzes to develop an effective discrete model, was adopted $SF = 1$.

The effect of the finite element mesh density

The next step of the sensitivity analysis was to determine of the effect of the finite element mesh density on the results of the calculations. In order to determine the object mapping tool and to set the maximum of the equivalent stress and strain of trapezoidal thread as a function of the density model variants were prepared with different numbers of finite elements. Calculations were performed for models that include the following number of finite elements $NFE = 220,\ 920,\ 3680,\ 8280,\ 22280, 32880$ and 45600. Table 2 summarizes the calculation options for $SF = 1$ for trapezoidal thread. For discretization was used the finite element PLANE183 type with 8-eight-nodes and non-linear shape function.

Tab. 3. The parameters of discrete effective models for trapezoidal and round threads

	Trapezoidal thread	**Round thread**
SF (shape factor)	1	1
NFE (number of FE)	32280	17640
NN (number of nodes)	99433	53317
NDOF (number degrees of nodes)	198866	106634
Finite element type	PLANE183	PLANE183

Influence of thread rolling conditions on the states of stress and strain in the round thread

Analyzing the distribution of deformation of the finite element grid and state of effective strains and stresses, presented in figures 13 and 14, where the influence of the lubrication condition is observed. For $\mu = 0$ in the contact zone tool – workpiece (Fig. 13a), during the forming the outline of the thread, material isn't braking by tool and slide through the contact surface. The curving of vertical line of the finite element grid is invisible. Other side, increase the friction coefficient causes increase braking of the material. For high value of the friction coefficient (Fig. 13c) occurs strong braking of material in the contact zone. Form also the adhesion zone of material. That cause higher displacements of material in the zone placed father from the contact zone. Then the line of the finite element grid are stronger curved.

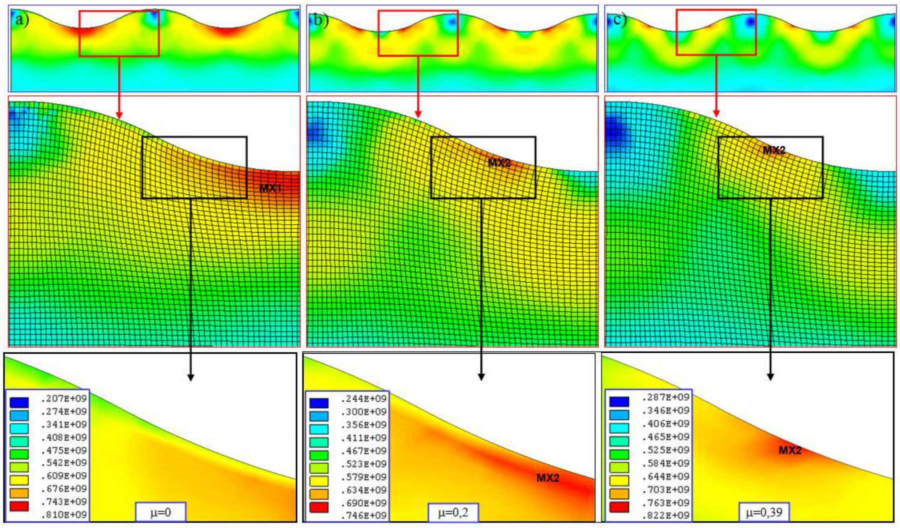

Fig. 13. *The deformation of grid and the maps of effective stresses in the thread on a longitudinal cutting plane for various value of frictions coefficient*

The friction coefficient has high influence on value and distribution of strain. For $\mu = 0$ the maximum of effective strain $\varepsilon_{eq} = 0,78$ is located on the bottom of the thread, near to the contact surface (MX1, Fig. 14a). For $\mu > 0$ appear an adhesion zone of material in the bottom of the thread, which take characteristic shape of a wedge. In this zone the value of strain is very small. For $\mu = 0,39$ strains are closer to the contact surface and getting smaller to value $\varepsilon_{eq} = 0,0016$ (elastic strains) (MN, Fig. 14b). Whereat the local maximum of strains (MX1) moving down in surface layer. Then appear additional two local maximums of the effective strains. Second maximum (MX2) is placed near to the contact zone of the side of the thread, where higher value of friction coefficient increase strains value from $\varepsilon_{eq} = 0,176$ for $\mu = 0$ (Fig. 14a) to value $\varepsilon_{eq} = 0,54$ for $\mu = 0,39$ (MX2, Fig. 14b). Next one local maximum (MX3) is located in depth of material on symmetry axis pass through top of the thread. Here, strains are getting smaller together with increasing of friction coefficient from value $\varepsilon_{eq} = 0,351$ for $\mu = 0$ (Fig. 14a) to $\varepsilon_{eq} = 0,423$ for $\mu = 0,39$ (Fig. 14b).

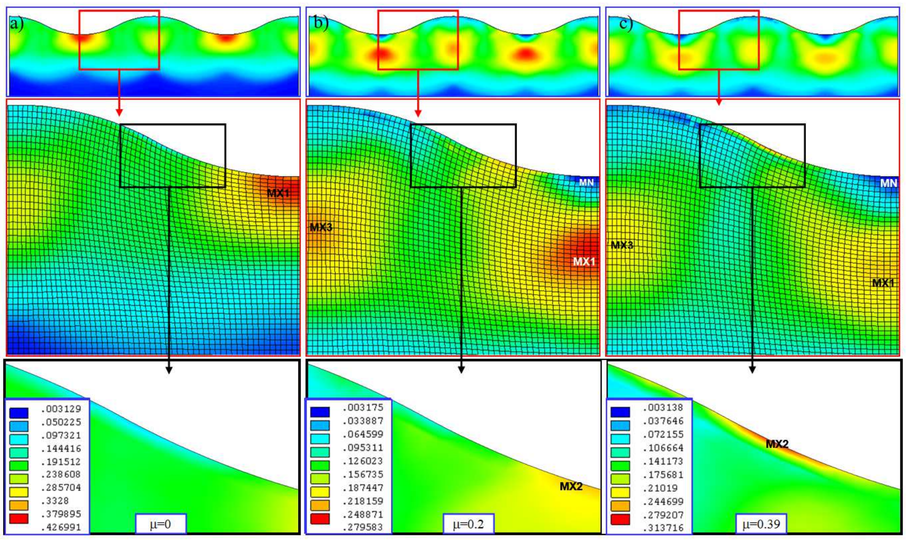

Fig. 14. *The maps of effective strains in the thread on a longitudinal cutting plane for various value of friction coefficient*

Figure 15 shows a comparison of the outline thread and the particle deformation (grid) (Fig. 15a), with the results of model studies (Fig. 15b) and results of numerical analysis according (Fig. 15c) and method II (Fig. 15d). Good agreement allows us to state that the effective discrete model for thread rolling is developed properly.

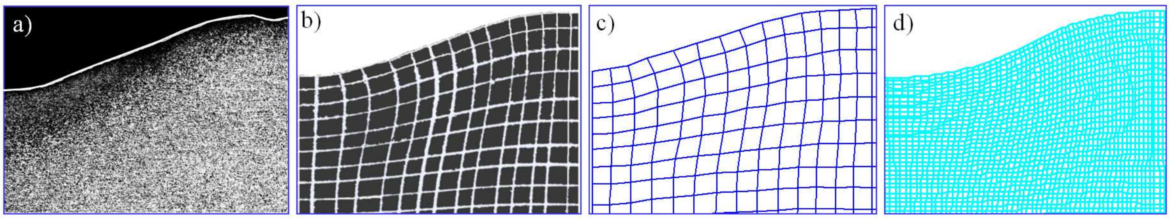

Fig. 15. *Comparison of experimental results (a, b) with the results of numerical calculations (c, d)*

6.3. Turning process [33]

For the correct modelling and analysis of the turning process, the knowledge of the course of the physical phenomena occurring in the machining zone in real conditions (i.e. geometry of tool and technological parameters) proves to be necessary. For this purpose, an analysis of the process of turning was conducted. The model of tool is considered as rigid or elastic body. The object is considered as the elastic/visco-plastic body (isothermal process). Numerical simulation in the ANSYS system was conducted for four different materials (failure strain $\varepsilon_f = 1,5;\ 2;\ 2,75;\ 4$) and four turning speed: $v = 40;\ 80;\ 160;\ 300$ m·s^{-1}. The object machined and the tool were digitized by elements of PLANE162 type with a non-linear function of shape. The contact tool with body was modelling by Single Surface Auto 2D (ASS2D). The net of finished elements was concentrated in the contact area. Sample simulation results are presented in Figs. 15 and 16.

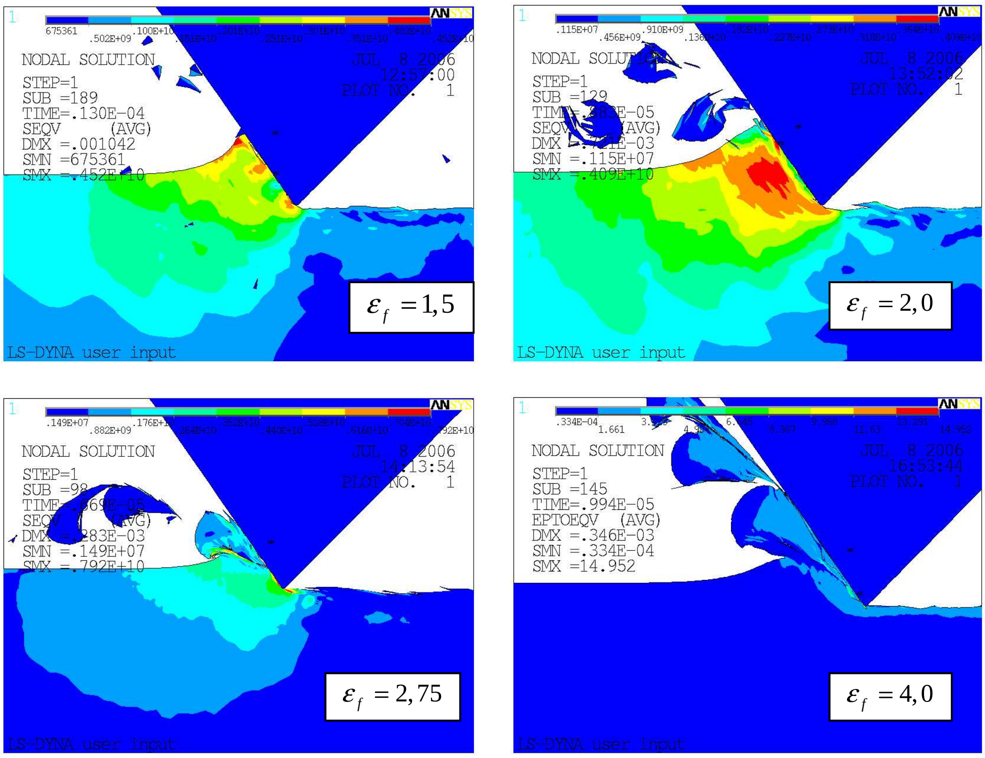

Fig. 15. *Chip geometry and maps of effective stress during turning process for different material steel [33]*

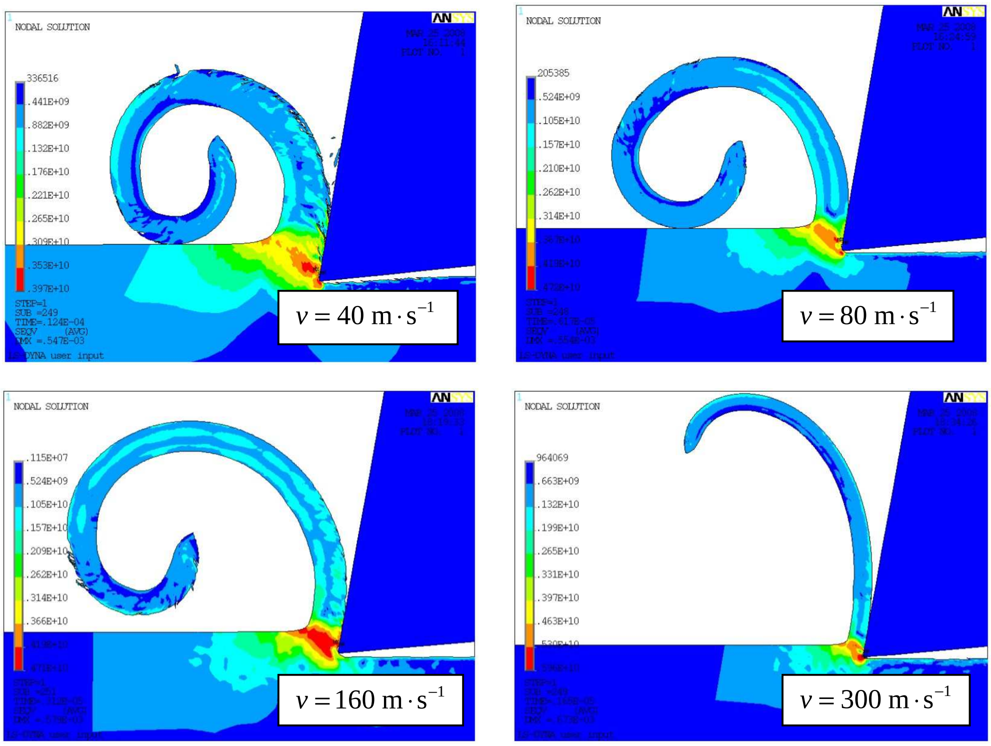

Fig. 16. *Chip geometry and maps of effective stress during turning process for different turning speed $v = 40; 80; 160; 300\ \mathrm{m \cdot s^{-1}}$ [33]*

The numerical results were compared with experimental results (Figs. 17-19).

a) *b)*

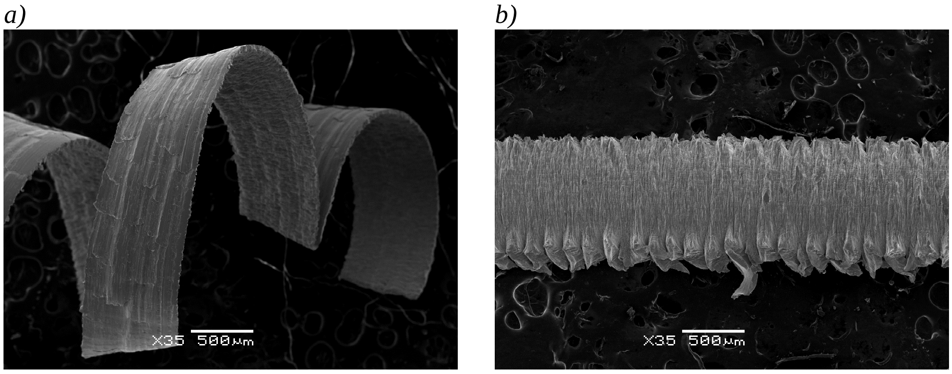

Fig. 17. *Fragments of a single chip of the screw (a) with a part of its outer surface (b) [57]*

a) *b)*

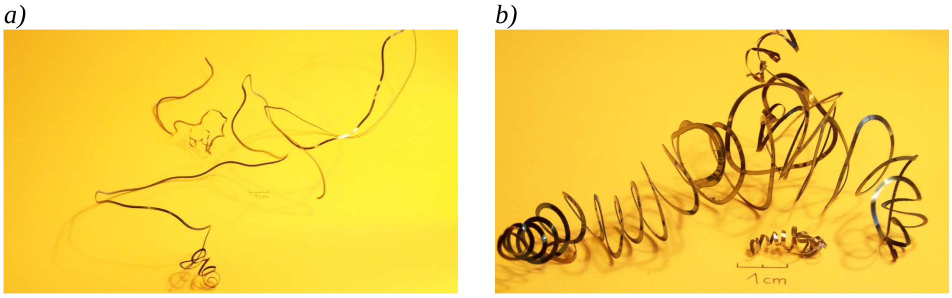

Fig. 18. *Chips long strip (a) and the screw open long (b) [57]*

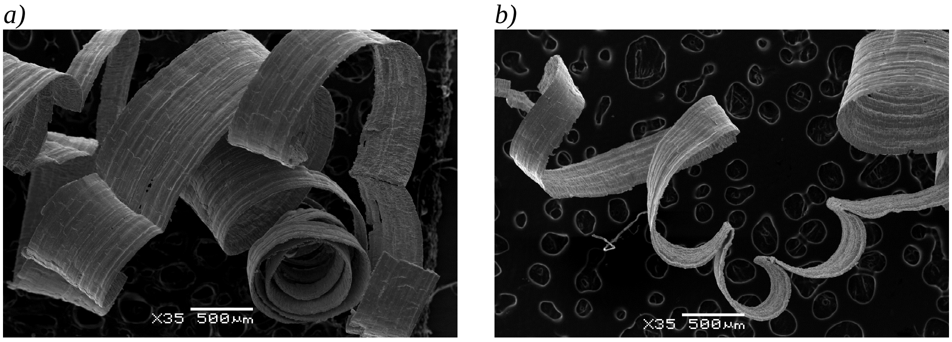

Fig. 19. *View of a portion of the helical chip (s) and the associated arc chip (b) [57]*

7. CONCLUSIONS

The paper presents a possibility of applying the variational and finite element methods for the analysis of physical phenomena in the technological processes.

The technological processes are geometrical, physical and thermal non-linear initial and boundary problem. Boundary conditions in the contact zone tool-object are not known. Measurement of a process parameters decide on the technological quality, such as: displacement, strain, stress, etc. during the process with nowadays technique of a measurement is impossible. About their course, we could conclude on the property of the product.

An application of modern mathematical modelling, numerical methods and computing systems allows an analysis of complex physical phenomena occurring in the process under investigation. The update Lagranian description has been used to describe nonlinear phenomena, on a typical incremental step. The states of strain and strain rate have been described by mean of nonlinear dependence without any linearization. The proper measures of strain and stress increments, i.e. the increment of Green-Lagrange's strain tensors and the increment of the second symmetric Pioli-Kirchhoff's strain tensors were applied. The nonlinearity of the material was described using the incremental model, making allowance for the effects of strain history and strain rate, and temperature. The workpieces have been considered treating an object as a body which can undergo thermo-elastic strains (in the range of reversible strain), thermo, viscous, plastic and phases (in the range of permanent strains). This body (thermo-elastic/thermo-visco-plastic-phases) has been designated as TE/TVPF. The material model was prepared making use of Huber-Mises-Hencky's nonlinear condition of plasticity, the associated law of flow and the mixed (isotropic-kinematical) strain hardening. The state of material after pre-processing was also taken into consideration introducing the initial conditions of displacements, strains, stresses and their rates. The incremental contact model obtained comprises the contact forces, contact rigidity, contact boundary conditions and friction conditions in this area. Then, the incremental functionals of the total system energy or entropy, were derived. From stationary condition of these functionals derived variational, nonlinear equation of motion and heat transfer for object on the typical incremental step time. These equations has been solved with finite elements spatial discretization, where the discrete system of motions and deformations equations of objects in the technological processes, were recived. The applications developed in the ANSYS system enables a time analysis of the technological processes with the consideration of the changeability of the lubrications conditions. On the course of physical phenomena in the working zone we can forecast a technological quality of the product.

The examples demonstrate the possibilities of numerical calculation of the developed method. Using mathematical incremental models, step-by-step numerical algorithm and we can perform a comprehensive analysis of thermal phenomena during the process of burnishing, even if we only partially know the temperature boundary conditions (knowledge of the temperature distribution in the contact zone object and tool is unknown). We can determine the temperature distribution and the distribution of heat fluxes for data of the initial state of the object, the pre-treatment conditions and the conditions of burnishing, or vice versa - to the desired temperature, we can determine the initial state of the object and conditions for implementing the pre-treatment and burnishing.

The obtained results of the computer simulation of the thread rolling process show that the friction coefficient influence on the states of displacements, strains and stresses in the surface layer of the thread, also is one of the factors deciding about the technological and the exploitation quality. The best operational quality of the thread is received during the rolling process on great lubrication conditions ($\mu = 0$). The simulation results for condition of lubrication can be use of while to designing the round thread rolling process: making a selection of the process condition and kind of the lubrication factor in the aspect of the technological quality of the thread.

The distributions of stresses obtained for different turning conditions, can be used of while designing machining: making a selection of the machining conditions and its optimising in the aspect of the technological quality of the product.

Good agreement numerical results with experimental results allows us to state that the effective discrete models were developed properly.

The methodology can be applied to the calculation of the state of strain, stress and temperature fields in other metal forming processes such as embossing of regular asperities before burnishing or thread rolling with electro contact heating and other technological processes i.e.: cutting processes, turning processes, burnishing rolling processes, cutting by an abrasive single grain, embossing, thread rolling, duplex burnishing, sliding burnishing and shot penning.

8. REFERENCES

[1] Przybylski W.: *Obróbka nagniataniem. Technologia i oprzyrządowanie*. WNT, Warszawa 1979.
[2] Przybylski W.: *Technologia obróbki nagniataniem*. WNT, Warszawa 1987.
[3] Kukiełka L.: *Theoretical and experimental foundations of surface roller burnishing with the electrocontact heating*, Book of Mechanical Engineering. Technical University of Koszalin No 47, Koszalin 1994, pp. 348.
[4] Martin J.A.: *Mesh density study for application to large deformation rolling process evaluations*, American Society of Mechanical Engineers, 373, 1998, pp. 177-184.
[5] Martin J.A.: *Fundamental Finite element evaluation of a three dimensional rolled thread form: modeling and experimental results*, American Society of Mechanical Engineers, 373, 1998, pp. 457-467.
[6] Kukiełka L: *Modelling of thermodynamical yield stress of metals dependent of the deformation history*, in: *Modern techniques and technology*, ZN WM, 29, Koszalin University of Technology, 2001, pp. 153-163.
[7] Kukielka L: *Incremental model of strain and stress of metals in the conditions of burnishing rolling operation*, in: Modern techniques and technology, ZN WM, 29, Koszalin University of Technology, 2001, pp. 174-191.
[8] Kukielka L.: *Mathematical modelling and numerical simulation of non-linear deformation of the asperity in the burnishing cold rolling operation*. Ed. Dominguez, J; Brebbia, CA Computational methods in contact mechanics V Book Series: Computational and experimental methods Vol. 5, 2001, pp. 317-326.
[9] Domblesky J.P., Feng F.: *A parametric study of process parameters in external thread rolling*, Journal of Materials Processing Technology, 121, 2002, pp. 341-349.
[10] Domblesky J.P., Feng F.: *Two-dimensional and three-dimensional finite element models of external thread rolling*, Professional Engineering Publishing, 216, 4, 2002, pp. 507-517.
[11] Kukiełka L.: *Basis of engineering researches*, PWN, Warsaw, 2002 (in Polish).
[12] Kukielka L., Kustra J.: *Numerical analysis of thermal phenomena and deformations in processing zone in the centreless continuous grinding process*, Computation Methods and Experimental Measurements for Surface Treatment Effects, WIT*PRESS*, Southampton, Boston, 2003, pp.109-118.
[13] Pater Z., Gontarz A., Weronski W: *New method of thread rolling*, Journal of Materials Processing Technology, 153–154, 2004, pp. 722-728.
[14] Kukielka L., Kustra J., Kukielka K.: *Numerical analysis of states of strain and stress of material during machining with a single abrasive grain*, in: J.T.M. de Hosson, C.A. Brebbia, S-I Nishida, Computer Methods and Experimental Measurements for Surface Effects and Contact Mechanics VII, WIT*PRESS*, Southampton-Boston, 2005, pp. 57-66.
[15] Kukielka K., Kukielka L.: *Modeling And Numerical Analysis Of The Thread Rolling Process*, WILEY-VCH Verlag GmbH & Co. KGaA, Vol. 6, Issue 1, 2006, pp. 745-746.
[16] Kukielka L., Kukielka K.: *Numerical analysis of the process of trapezoidal thread rolling*, in: C.A. Brebbia (Eds.), High Performance Structures and Materials III, WIT*PRESS*, Southampton-Boston, 2006, pp. 663-672.
[17] Kułakowska A.: *Wpływ odchyłek zarysu regularnych nierówności powierzchni po obróbce toczeniem na wybrane właściwości warstwy wierzchniej wyrobu nagniatanego tocznie.* Praca doktorska. Koszalin, 2006
[18] Kukielka L., Kukielka K.: *Numerical analysis of the physical phenomena in the working zone in the rolling process of the round thread*, in: J.T.M. de Hosson, C.A. Brebbia, S-I Nishida, Computer Methods and Experimental Measurements for Surface Effects and Contact Mechanics VIII, WIT*PRESS*, Southampton-Boston, 2007, pp. 125-124.
[19] Chodór J., Kukiełka L.: *Numerical analysis of the influence of abrasive grain geometry and cutting angle on states of strain and stress in the surface layer of object*, Surface/Contact Conference, Wessex Institute, Ashurst Lodge, Ashurst, Southampton, UK, 2007.
[20] Kukiełka L., Chodór J.: *Numerical analysis of chip formation during machining for different value of failure strain*, Journal PAMM, Vol. 7, Issue 1, 2008, pp. 4030031-4030032.

[21] Chodór J., Kukiełka L.: *Numerical analysis of micromachining of C45 steel with single abrasive grain*. GAMM 79th Annual Meeting of the International Association of Applied Mathematics and Mechanics, 31 March – 4 April, Bremen 2008.
[22] Kulakowska A., Kukielka L.: *Numerical analysis and experimental researches of burnishing rolling process with taking into account deviations in the surface asperities outline after previous treatment*. Steel Res. Int. 2, 2008, pp. 42-48.
[23] Patyk R., Kukielka L.: *Optimization of geometrical parameters of regular triangular asperities of surface put to smooth burnishing*, The 12th International Conference Metal Forming 2008, Steel Research International, 2, Kraków, 2008, pp. 642-647.
[24] Forysiewicz M., Chodór J., Kukiełka L.: *Modelowanie dyskretne i analiza numeryczna procesu skrawania pojedynczym ziarnem ściernym metodą elementów skończonych*. Obrabiarki sterowane numerycznie i programowanie operacji w technikach wytwarzania. Zakład Poligraficzny Politechniki Radomskiej, Radom 2009.
[25] Chodór J., Kukiełka L., Storch B.: *New method of determination of tool rake angle on the basis of crack angle of specimen in tensile test and numerical simulations*. Ninth International Conference on Surface Effects and Contact Mechanics Computational Methods and Experiments, Algarve, Portugal, 2009.
[26] Kukiełka K.: *Modelling and numerical analysis of the states of deformations and stresses in the surface layer of the trapezoidal and round threads rolled on cold*, PhD Thesis, Koszalin University of Technology, 2009. (in Polish)
[27] Kałduński P.: *Modelowanie i symulacja kształtowania wytłoczek kołowo symetrycznych bez kołnierza z uwzględnieniem nieliniowości geometrycznej i fizycznej*. Praca doktorska, Koszalin, 2009.
[28] Kukielka L., Kulakowska A., Patyk R.: *Numerical Modeling and Simulation of the Movable Contact Tool-Worpiece and Application in Technological Processes*, The 13th World Multi-Conference on Systemics, Cybernetics and Informatics, Orlando, Floryda 2009, pp. 57-62.
[29] Kulakowska A., Patyk R., Kukielka L.: *Numerical analysis and experimental researches of burnishing rolling process of workpieces with real surface*, WMSCI 2009 – The 13th World Multi-Conference on Systemics, Cybernetics and Informatics, Jointly with the 15th International Conference on Information Systems Analysis and Synthesis, ISAS 2009 – Proc. Volume 2, 2009, pp. 63-68.
[30] Patyk R.: *Theoretical and experimental basis of regular asperities about triangular outline embossing technology*, The 13th International Conference Metal Forming 2010, Steel Research International, 81, Toyohashi, 2010, 190-193.
[31] Kukielka L.: *New damping models of metallic materials and its application in non-linear dynamical cold processes of metal forming*, Steel Research International, 81, 2010, pp. 1482 –1485.
[32] Kulakowska A.: *Problems of surface preparation under burnishing rolling in aspect of product quality*. Steel Research International vol. 81/9, 2010, pp. 218-221.
[33] Chodór J.: *Modelowanie i analiza przemieszczania materiału obrabianego podczas mikroskrawania i nagniatania ślizgowego z uwzględnieniem nieliniowości procesu*. Rozprawa doktorska. Koszalin, 2011.
[34] Chodór J., Forysiewicz M., Kukiełka L.: *Analiza numeryczna tworzenia wypływki i wióra dla sprężysto-/lepko-plastycznego podłoża w procesie przemieszczania klina*. XXXIV Naukowa Szkoła Obróbki Ściernej, Gdańsk 2011.
[35] Kukiełka K.: Czterorolkowa głowica kątowa do walcowania gwintów o zarysie łukowym na rurach i wałkach. Współczesne problemy w technologii obróbki przez nagniatanie, Politechnika Gdańska, 2011, s. 433-448.
[36] Kukiełka L., Bohdal Ł., Chodór J., Forysiewicz M., Geleta K., Kałduński P., Kukiełka K., Patyk R., Szyc M.: *Analiza numeryczna wybranych procesów technologicznych precyzyjnej obróbki części samochodowych*. Ekologiczne aspekty stosowania nowych technologii w transporcie. Monografia nr 235 Wydziału Mechanicznego, Politechniki Koszalińskiej, pod redakcją Leona Kukiełki, Koszalin, 2012, s. 129-194.
[37] Bohdal Ł., Kukiełka L.: *Modelowanie i analiza numeryczna procesu cięcia blach nożami krążkowymi z uwzględnieniem nieliniowości geometrycznej i fizycznej*. Mechanik 84, nr 8-9, 2011, s. 712÷716.
[38] Bohdal L.: *Finite element simulation of 3D sheet metal guillotining using elastic/visco-plastic damage model*, Steel Research International, 2012, pp. 1419-1422.
[39] Kukielka L., Geleta K., Kukielka K.: *Modelling and Analysis of Nonlinear Physical Phenomena in the Burnishing Rolling Operation with Electrical Current*, in: K. Mori, M. Pietrzyk, J. Kusiak, J. Majta, P Hartley, J. Lin (Eds.), Steel Research International. Special Edition: 14th International Conference Metal Forming, 2012, pp. 1379-1382.
[40] Kukielka L., Geleta K., Kukielka K.: *Modelling of Initial and Boundary Problems with Geometrical and Physical Nonlinearity and its Application in Burnishing Processes* in: K. Mori, M. Pietrzyk, J. Kusiak, J. Majta, P Hartley, J. Lin (Eds.), Steel Research International. Special Edition: 14th International Conference Metal Forming, 2012, pp. 1375-1378.

[41] Kukiełka L., Kukiełka K.: *Nowoczesna metoda modelowania i analizy procesów technologicznych precyzyjnej obróbki części samochodowych.* Ekologiczne aspekty stosowania nowych technologii w transporcie. Monografia nr 235 Wydziału Mechanicznego, Politechniki Koszalińskiej, pod redakcją Leona Kukiełki, Koszalin 2012, s. 109÷128.

[42] Szyc M.: *Modelowanie i symulacja procesu kształtowania struktury geometrycznej powierzchni części stalowych dynamicznym nagniataniem śrutem kulistym*. Rozprawa doktorska, Wydział Mechaniczny, Politechnika Koszalińska, Koszalin 2013.

[43] Gryglicki R.: *Modelowanie i optymalizacja procesu nagniatania ślizgowego elementem diamentowym wałków nawęglanych i hartowanych, na przykładzie stali 16HG.*. Rozprawa doktorska, Wydział Mechaniczny, Politechnika Koszalińska, Koszalin, 2013.

[44] Kukiełka K., Kukiełka L.: *Głowica do walcowania gwintów zewnętrznych*, Patent nr P 402652, z dnia 4.02.2013.

[45] Bohdal L., Walczak P.: *Eco-modeling of metal sheet cutting with disc shears*, Annual Set The Environment Protection 15, 2013, pp. 863-872.

[46] Kukielka L., Kukielka K., Kulakowska A., Patyk R., Malag L., Bohdal L.: *Incremental Modelling and Numerical Solution of the Contact Problem between Movable Elastic and Elastic/Visco-Plastic Bodies and Application in the Technological Processes*. Applied Mechanics and Materials *Novel Trends in Production Devices and Systems*, Editors: Karol Velíšek, Peter Košťál and Milan Nad, 2014, USA-SLOVAKIA, pp. 159-165. ISSN 1662-7482.

[47] Bohdal L., Kukielka L., Kukielka K., Kulakowska A., Malag L., Patyk R.: *Three Dimensional Finite Element Simulation of Sheet Metal Blanking Process*. Applied Mechanics and Materials *Novel Trends in Production Devices and Systems*, Editors: Karol Velíšek, Peter Košťál and Milan Nad, 2014, USA-SLOVAKIA, pp. 430-435. ISSN 1662-7482.

[48] Kukielka K., Kukielka L., Bohdal L., Kulakowska A., Malag L., Patyk R.: *3D Numerical Analysis the State of Elastic/Visco-Plastic Strain in the External Round Thread Rolled on Cold*. Applied Mechanics and Materials *Novel Trends in Production Devices and Systems*, Editors: Karol Velíšek, Peter Košťál and Milan Nad, 2014, USA-SLOVAKIA, pp. 436-441. ISSN 1662-7482.

[49] Kulakowska A., Kukielka L., Kukielka K., Patyk R., Malag L., Bohdal L.: *Possibility of Steering of Product Surface Layers Properties in Burnishing Rolling Process*. Applied Mechanics and Materials *Novel Trends in Production Devices and Systems*, Editors: Karol Velíšek, Peter Košťál and Milan Nad, 2014, USA-SLOVAKIA, pp. 442-447. ISSN 1662-7482.

[50] Patyk R., Kukielka L., Kukielka K., Kulakowska A., Malag L., Bohdal L.: *Numerical Study of the Influence of Surface Regular Asperities Prepared in Previous Treatment by Embossing Process on the Object Surface Layer State after Burnishing*. Applied Mechanics and Materials *Novel Trends in Production Devices and Systems*, Editors: Karol Velíšek, Peter Košťál and Milan Nad, 2014, USA-SLOVAKIA, pp. 448-453. ISSN 1662-7482.

[51] Malag L., Kukielka L., Kukielka K., Kulakowska A., Bohdal L., Patyk R.: *Problems Determining of the Mechanical Properties of Metallic Materials from the Tensile Test in the Aspect of Numerical Calculations of the Technological Processes*. Applied Mechanics and Materials *Novel Trends in Production Devices and Systems*, Editors: Karol Velíšek, Peter Košťál and Milan Nad, 2014, USA-SLOVAKIA, pp. 454-459. ISSN 1662-7482.

[52] Kaldunski P., Kukielka L.: *Numerical Analysis and Simulation of Drawpiece Forming Process by Finite Element Method*. Applied Mechanics and Materials *Novel Trends in Production Devices and Systems*, Editors: Karol Velíšek, Peter Košťál and Milan Nad, 2014, USA-SLOVAKIA, pp. 153-158. ISSN 1662-7482.

[53] Chodor J., Kukielka L.: *Using Nonlinear Contact Mechanics in Process of Tool Edge Movement on Deformable Body to Analysis of Cutting and Sliding Burnishing Processes*. Applied Mechanics and Materials *Novel Trends in Production Devices and Systems*, Editors: Karol Velíšek, Peter Košťál and Milan Nad, 2014, USA-SLOVAKIA, pp. 339-344. ISSN 1662-7482.

[54] Kukiełka K.: *Effective numerical model to analyze the trapezoidal thread rolling process with finite element method*. Mechanik No 11, 2014, pp. 156-167.

[55] Bohdal Ł.: *Zastosowanie przyrostowej metody analizy siatki koordynacyjnej do numerycznej analizy procesu cięcia*, Pomiary Automatyka Kontrola, Nr 10-12 2014 r. ISSN 0032-4140.

[56] Bohdal Ł.: *Badania eksperymentalne i symulacyjne procesu cięcia stopów aluminium nożycami krążkowymi*, Mechanik, nr 7/2014, ISSN 0025-6552, s. 534-539.

[57] Chodór J., Kukiełka L.: *Zastosowanie nieliniowej mechaniki kontaktu w analizie przemieszczania materiału obrabianego podczas skrawania i nagniatania ślizgowego*, Mechanik, nr 8-9/2014, ISSN 0025-6552, s. 23-30.

[58] Gryglicki R., Kukiełka L.: *Kształtowanie przeciwzużyciowej warstwy wierzchniej słupów nośnych form wtryskowych metodą nagniatania ślizgowego*, Mechanik nr 11/2014, ISSN 0025-6552, s. 111-117.

[59] Szyc M., Kukiełka L., Legutko S.: *Komputerowe wspomaganie procesu dynamicznego nagniatania śrutem kulistym*, Mechanik, nr 11/2014, ISSN 0025-6552, s. 236-253.

[60] Kułakowska A., Bohdal Ł., Patyk R.: *Zastosowanie obróbki nagniataniem w tworzeniu ekologicznego produktu*, Annual Set The Environment Protection, Vol. 16, 2014, ISSN 1506-218X.

[61] Patyk R., Kułakowska A., Bohdal Ł.: *Ekologiczne, ekonomiczne i eksploatacyjne aspekty obróbki nagniataniem*, Annual Set The Environment Protection, Vol. 16, 2014, ISSN 1506-218X, s. 351-362.

[62] Bohdal Ł., Kułakowska A., Patyk R.: *Analysis of slitting of aluminium body panels in the aspect of scrap reduction*, Annual Set The Environment Protection, Vol. 16, 2014, ISSN 1506-218X.

[63] Bohdal Ł., Kukiełka L.: *Application of variational and FEM methods to the modelling and numerical analysis of slitting process for geometrical and physical nonlinearity*, Journal of Theoretical Applie Mechanics, ISSN 1392-1207, Mechanika, 2014 Vol. 20(2), s. 197-204.

[64] Szyc M., Kukiełka L., Kukiełka K., Gotowała K.: *Analiza zjawisk fizycznych w przedmiocie podczas dynamicznego nagniatania śrutem kulistym*, Współczesne problemy w technologii obróbki przez nagniatanie, TOM 4, Monografia, Politechnika Gdańska, ISBN : 978-83-941224-0-9, 2014, s. 44-58.

[65] Kukiełka K., Kukiełka L.: *A modern methodology to modelling and analysis of technological metals treatment processes*. Modelowanie Warstwy Wierzchniej Monografia, pod red. naukową. prof. dr hab. dr h.c. inż. Tadeusza Zaborowskiego, Gorzów Wlkp., 2014, s. 6-25. ISBN 978-83-64249-11-2. Wydawca IBEN Gorzów Wlkp. 2014.

[66] Bohdal Ł., Kukiełka K., Kułakowska A., Patyk R.: *Finite element simulation of sheet metal guillotining: study of guillotining parameters on sheared edge quality*. Modelowanie Warstwy Wierzchniej Monografia, pod red. naukową. prof. dr hab. dr h. c. inż. Tadeusza Zaborowskiego, Gorzów Wlkp., 2014, s. 198-209, ISBN 978-83-64249-11-2. Wydawca IBEN Gorzów Wlkp. 2014.

[67] Kukiełka K., Bohdal Ł., Kułakowska A., Patyk R.: *Using 3D numerical analysis to determine influence of the technological parameters on the rolled thread quality*. Warstwa Wierzchniej Monografia, pod red. naukową. prof. dr hab. dr h.c. inż. Tadeusza Zaborowskiego, Gorzów Wlkp., 2014, str. 52-65, ISBN 978-83-64249-11-2, Wydawca IBEN Gorzów Wlkp. 2014.

[68] Chodór J. Kałduński P.: Experimental researches of influence of sliding burnishing technological conditions for surface roughness of 41CR4 steel product, Modelowanie Warstwy Wierzchniej Monografia, pod red. naukową. prof. dr hab. dr h.c. inż. Tadeusza Zaborowskiego, Gorzów Wlkp., 2014, s. 226-241, ISBN 978-83-64249-11-2, Wydawca IBEN Gorzów Wlkp. 2014.

[69] Kałduński P. Chodór J: *Numerical analysis of the deep drawing process by finite element method for anisotropic model of object*, Modelowanie Warstwy Wierzchniej Monografia pod red. naukową prof. dr hab. dr h. c. inż. Tadeusza Zaborowskiego, Gorzów Wlkp., 2014, s. 40-51, ISBN 978-83-64249-11-2, Wydawca IBEN Gorzów Wlkp. 2014.

[70] Patyk R., Kułakowska A., Bohdal Ł., Kukiełka K.: *The numerical analysis of sensibility of embossing process of regular asperities of surface on the material parameters of work-pieces in aspect of surface layer quality*. Modelowanie Warstwy Wierzchniej, Monografia pod red. naukową prof. dr hab. dr h. c. inż. Tadeusza Zaborowskiego, Gorzów Wlkp., 2014, s. 269-281, ISBN 978-83-64249-11-2, Wydawca IBEN Gorzów Wlkp. 2014.

[71] Kułakowska A., Patyk R., Bohdal Ł., Kukiełka K.: *Surface layer after burnishing rolling of the rough surface*. Modelowanie Warstwy Wierzchniej, Monografia pod red. naukową prof. dr hab. dr h. c. inż. Tadeusza Zaborowskiego, Gorzów Wlkp., 2014, s. 242-253, ISBN 978-83-64249-11-2, Wydawca IBEN Gorzów Wlkp. 2014.

[72] Forysiewicz M.: *Analiza stanów deformacji i naprężeń w strefie obróbki materiałów sprężysto-lepko-plastycznych podczas szybkościowego skrawania pojedynczym ostrzem*. Rozprawa doktorska. Koszalin, 2015.

[73] Patyk S.: *Analiza sił nagniatania tocznego powierzchni chropowatych o trójkątnym zarysie nierówności*. Rozprawa doktorska, 2015.

[74] Bohdal Ł., Gotowała K.: *Numerical and experimental analysis of the tool geometry on states of stresses and strains during shear slitting of aluminum alloys*, (in polish) (in this journal).

[75] Chodór J., Zurawski Ł.: *Researches of chip shape and its swage factor and shortening factor in partial symmetric face milling process and simulation of the process using FEM* (in polish) (in this journal).

[76] Kukiełka L., Szcześniak M.: *Influence of the apex angle of triangular asperities of surfaces after previous treatememnt on the roughness of the surface after squeezing process* (in polish) (in this journal).

[77] Patyk R., Patyk S., Kukiełka L.: *Determination of the principal burnishing force roller rouhnes surface with regular periodical outlines asperities using numerical methods* (in polish) (in this journal).

[78] Patyk R., Patyk S., Kukiełka L.: *Determining contact pressures during embossing process of regular asperities on the cylindrical surfaces* (in polish) (in this journal).

[79] Bathe K.J.: *Finite Element Procedures in Engineering Analisis*, Prentice – Hall, Englewood Cliffs, N.J., 1982.

[80] Kleiber M, *Finite element method in non-linear solid mechanics*, PWN, Warsaw, 1985 (in Polish).

[81] Zienkiewicz O.C., Taylor R. L.: *The finite element method*, Volume 1 – The Basis, Butterworth-Heinemann, United Kingdom, 2000.